北九州市立大学
THE UNIVERSITY OF KITAKYUSHU

DOSY NMR: A Valuable Tool for Determining the Enhanced Binding Constant of Cyclodextrin Nanoparticles

Doan Thi Ngoc Anh

Supervisor: Professor Kazuo Sakurai

A thesis submitted for the fulfilment of the requirements for the degree of

Doctor of Engineering

Graduate School of Environmental Engineering

The University of Kitakyushu

June 2024

Abstract

This thesis investigates the profound impact of polymerization on the binding affinity of cyclodextrin (CD)-based nanoparticles (CDNPs) with various drug molecules. By incorporating epichlorohydrin (ECH) into CDNPs, the binding constants between CDs and drug compounds are significantly enhanced. Utilizing Diffusion-Ordered Spectroscopy Nuclear Magnetic Resonance (DOSY NMR) as a key analytical tool, the study delves into the mechanisms governing the enhanced binding affinity. Through a series of experiments employing DOSY NMR and other methodologies, the thesis elucidates the mechanisms underlying this enhanced binding affinity.

Our study reveals a significant enhancement in the binding affinity between CDs and various drugs, particularly exemplified by the interaction between alpha-mangostin (MGS) and CDs within ECH-incorporated nanoparticles. Employing a 1:1 association model, we evaluate the binding constant, witnessing an approximately 100-fold increase. Furthermore, polymerization of CD with ECH dramatically elevates the binding constant with vanillin, suggesting the pivotal role of ECH hydrophobicity in enhancing binding.

Expanding our investigation, we explore the interaction between paroxetine hydrochloride (PRX) and βCD or βCDNP, showcasing superior binding affinity within the polymer matrix. Notably, the formation of a 2:1 βCD-PRX inclusion complex within the polymer hints at enhanced drug delivery potential, particularly for enhancing solubility and stability of hydrophobic drugs. These findings contribute to the understanding of host-guest interactions, with implications for optimizing therapeutic outcomes.

Moreover, the study explores the potential applications of these enhanced binding interactions in drug delivery systems, particularly in improving the solubility and stability of hydrophobic drugs. The investigation further extends to assessing the biocompatibility and safety profiles of CDNPs, demonstrating their potential for mitigating nephrotoxicity commonly associated with CDs.

The thesis underscores the significance of supramolecular chemistry in advancing drug delivery systems, offering valuable insights into host-guest interactions and their implications for therapeutic efficacy. By elucidating the molecular mechanisms governing the interactions between CDNPs and drug molecules, the study contributes to the development of more effective drug delivery strategies, with the potential to enhance patient outcomes. Overall, the research presented in this thesis advances our understanding of cyclodextrin-based nanotechnology and its applications in pharmaceutical sciences.

Thesis including published works declaration

I hereby declare that this thesis contains no material which has been accepted for the award of any other degree or diploma at any university or equivalent institution and that, to the best of my knowledge and belief, this thesis contains no material previously published or written by another person, or any use of generative artificial intelligence technologies, except where due reference is made in the text of the thesis.

This thesis includes 2 original papers published in peer reviewed journals and 1 accepted publication. The ideas, development and writing up of all the papers in the thesis were the principal responsibility of myself, the student, working within the University of Kitakyushu under the supervision of Professor Kazuo Sakurai. The inclusion of co-authors reflects the fact that the work came from active collaboration between researchers and acknowledges input into team-based research.

Thesis chapter	Publication title	Single or joint authorship	Status	Date of issuance or publication	Name of the publisher, journal, academic conference or society; Vol., No., p.p.
2	[Peer-reviewed papers in journals] 1. Dramatically Increased Binding Constant of Water-Soluble Cyclodextrin Hyperbranched Polymers: Explored with Diffusion Ordered NMR Spectroscopy (DOSY) (Anh Thi Ngoc Doan, Van Thi Hong Doan, Jun Katsuki, Shota Fujii, Hiroyuki Kono, and Kazuo Sakurai)	Joint authorship	Published	March, 2022	ACS Omega, Volume 7, Issue 13, Pages 10890-10900 doi.org/10.1021/acsomega.1c06194
3	2. Unraveling the molecular mechanism of the interaction between cyclodextrin-based nanoparticles (CDNPs) and paroxetine hydrochloride (Anh Thi Ngoc Doan, Kazuo Sakurai)	Joint authorship	Published	April, 2024	Bulletin of the Chemical Society of Japan, Volume 97, Issue 4, uoae042 doi.org/10.1093/bulcsj/uoae042
4, 5	3. Reduced nephrotoxicity of epichlorohydrin-crosslinked	Joint authorship	Accepted		Journal of Bioactive and Compatible Polymers

	β-cyclodextrin nanoparticles (βCDNPs) and its enhanced binding with hydrophobic compounds (Anh Thi Ngoc Doan, Natsuki Kojima, Kazuo Sakurai)				

Acknowledgements

I would like to express my deepest gratitude to Professor Kazuo Sakurai for his invaluable guidance, support, and encouragement throughout my research. His expertise and advice have been instrumental in the completion of this thesis.

I extend my sincere thanks to Dr. Doan Thi Hong Van for her patience and dedication in guiding me through the laboratory work.

I am also grateful to Natsuki Kojima for her assistance with the in vivo experiments, which were crucial for the success of this research.

I would like to thank the Ministry of Education, Culture, Sports, Science and Technology (MEXT) of Japan for providing me with the scholarship that made this research possible.

Finally, I am immensely thankful to my family and friends for their unwavering support and encouragement, which has been a constant source of strength for me.

Table of Contents

List of figures

List of tables

Chapter 1. Introduction

1-1. Introduction to cyclodextrins (CDs)

Cyclodextrins (CDs) are a unique class of cyclic oligosaccharides derived from starch through the enzymatic activity of cyclodextrin glycosyltransferase (CGTase). These molecules are composed of glucose units linked by α-1,4-glycosidic bonds, forming a ring structure. The most commonly studied and utilized CDs are α-cyclodextrin (αCD), β-cyclodextrin (βCD), and γ-cyclodextrin (γCD), which consist of six, seven, and eight glucose units, respectively as shown in Figure 1-1. Each type of CD has distinct physical and chemical properties that make them suitable for various applications.

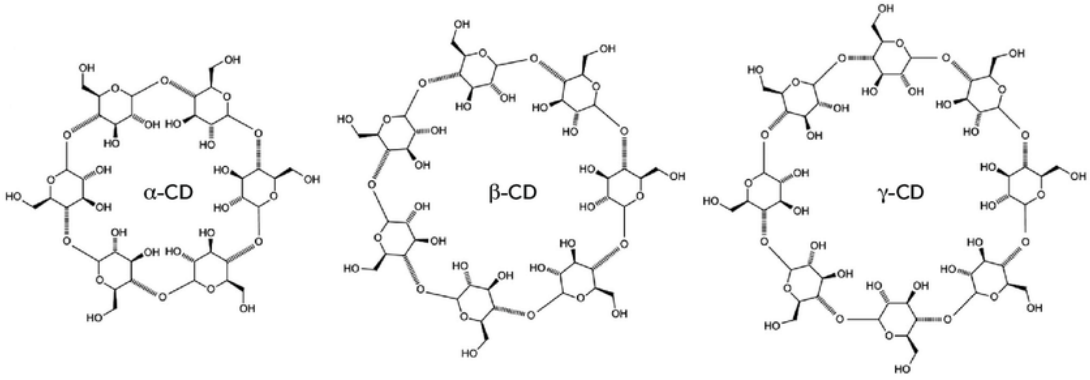

Figure 1-1. Chemical structure of cyclodextrins.

The molecular architecture of CDs is characterized by a toroidal or truncated cone shape. This unique structure imparts CDs with a hydrophilic outer surface and a hydrophobic inner cavity. The hydrophilic exterior is due to the presence of hydroxyl groups on the glucose units, which interact readily with water molecules. In contrast, the hydrophobic interior is formed by the non-polar faces of the glucose rings, creating an ideal environment for encapsulating hydrophobic molecules. [2]

One of the most significant properties of CDs is their ability to form inclusion complexes. The hydrophobic cavity of CDs can host a variety of guest molecules, ranging from small organic compounds to parts of larger biomolecules. This inclusion complexation significantly enhances the solubility, stability, and bioavailability of guest molecules, particularly hydrophobic substances that are

otherwise poorly soluble in water. The non-covalent nature of these interactions, including Van der Waals forces, hydrophobic interactions, and hydrogen bonds, allows for the reversible encapsulation and release of guest molecules. [2]

Cyclodextrins are naturally occurring, albeit in trace amounts, in certain fermented foods and beverages such as beer, bread, and other products derived from starch. For industrial and research purposes, CDs are typically produced on a larger scale through the enzymatic conversion of starch by CGTase. This enzymatic process is both efficient and scalable, allowing for the commercial production of high-purity CDs.

1-2. Applications of cyclodextrins (CDs)

Cyclodextrins (CDs) have garnered significant attention and found diverse applications across various industries due to their unique molecular properties. From pharmaceuticals to environmental science, CDs offer solutions to challenges related to solubility, stability, and delivery of bioactive compounds. [3] Here are some key applications of cyclodextrins:

Pharmaceutical industry:

- Solubilization of hydrophobic drugs: CDs are widely employed to enhance the solubility and bioavailability of poorly water-soluble drugs. By forming inclusion complexes with hydrophobic drug molecules, CDs improve their dissolution rates, facilitating better absorption and efficacy. [4]

- Controlled drug release: The encapsulation of drugs within cyclodextrin complexes allows for controlled release formulations. CDs provide a protective environment for the drug molecules, controlling their release kinetics and prolonging therapeutic effects. [5, 6]

- Stabilization of labile compounds: Labile drugs, prone to degradation or oxidation, benefit from encapsulation within cyclodextrins. CDs shield these compounds from environmental factors, preserving their stability and extending shelf life. [7]

Food and beverage industry

- Flavor and fragrance encapsulation: Cyclodextrins are utilized to encapsulate volatile flavor and fragrance compounds, protecting them from degradation and evaporation. This application enhances the stability and longevity of flavors and fragrances in food products and beverages.[8, 9]

- Nutrient delivery: CDs are employed to encapsulate vitamins, antioxidants, and other bioactive compounds in food and dietary supplements. This enhances the solubility and bioavailability of these nutrients, ensuring their effective delivery to the body.[10 11]

Cosmetics and personal care products

- Stabilization of active ingredients: Active ingredients in cosmetics and personal care products, such as anti-aging compounds and sunscreens, are often encapsulated within cyclodextrins. This protects these ingredients from degradation caused by exposure to light, air, and other environmental factors. [12]

- Enhanced skin penetration: CDs facilitate the delivery of active ingredients into the deeper layers of the skin by forming inclusion complexes. This improves the efficacy of skincare products and enhances their ability to target specific skin concerns. [13]

Environmental remediation

- Pollutant removal: Cyclodextrins are employed in environmental remediation efforts to remove organic pollutants from water and soil. CDs form complexes with pollutants, effectively sequestering them and preventing their migration or leaching into the environment. [14]

- Heavy metal sequestration: CDs have been studied for their ability to complex with heavy metal ions, facilitating their removal from contaminated environments. This application contributes to efforts aimed at mitigating the environmental impact of heavy metal pollution. [15]

Analytical chemistry

- Chromatographic separation: CDs are utilized as stationary phases in chromatographic techniques for the separation and analysis of complex mixtures.

The selective complexation properties of CDs enable the isolation and identification of specific analytes from complex matrices. [16]

- Drug assay development: CDs are employed in drug assay development to enhance the sensitivity and specificity of analytical methods. By forming inclusion complexes with target analytes, CDs improve detection limits and accuracy in pharmaceutical analysis. [17]

Agriculture

- Enhanced delivery of agrochemicals: Cyclodextrins are used to encapsulate pesticides, herbicides, and fertilizers, enhancing their solubility and efficacy. This improves the targeted delivery of agrochemicals to plants, reducing environmental contamination and optimizing crop yields. [18]

- Soil remediation: CDs have shown promise in soil remediation applications by facilitating the encapsulation and removal of organic contaminants. This contributes to the restoration of polluted soils and ecosystems, supporting sustainable agricultural practices. [19]

Other applications

- Textile industry: CDs are employed in the textile industry for dye encapsulation and color retention. This improves the durability and colorfastness of textiles, enhancing their aesthetic appeal and longevity. [20]

- Medical evices: Cyclodextrins are utilized in the design of medical devices and biomaterials for drug delivery and tissue engineering applications. CDs impart controlled release properties to implantable devices, ensuring precise dosing and therapeutic outcomes. [21]

The versatility of CDs has led to extensive research aimed at modifying their structures to enhance their functional properties. Chemical modifications, such as the introduction of various substituents on the hydroxyl groups, have produced derivatives with tailored solubility, stability, and binding affinities. These modifications expand the potential applications of CDs and enable the

development of more sophisticated drug delivery systems, environmental remediation strategies, and other advanced technologies.

In conclusion, cyclodextrins are versatile molecules with a wide range of applications across diverse industries. From improving drug delivery in pharmaceuticals to remediation of environmental pollutants, CDs continue to drive innovation and address critical challenges in various fields. Ongoing research and development efforts are expected to further expand the utility and effectiveness of cyclodextrins in solving complex problems and advancing technological solutions.

1-3. Pharmaceutical applications of cyclodextrins

Cyclodextrins (CDs) play a pivotal role in the pharmaceutical industry, offering versatile solutions to various challenges encountered in drug development, formulation, and delivery. Their unique molecular structure and properties make them indispensable in enhancing the solubility, stability, and bioavailability of poorly water-soluble drugs. Here are some key pharmaceutical applications of cyclodextrins:

Solubility enhancement

- Encapsulation of hydrophobic drugs: CDs are renowned for their ability to form inclusion complexes with hydrophobic drug molecules, thereby improving their aqueous solubility. This solubilization enables the formulation of drug products with higher concentrations and facilitates drug administration via various routes, including oral, parenteral, and topical. [22]

- Dissolution rate enhancement: By increasing the solubility of poorly water-soluble drugs, CDs enhance their dissolution rates, leading to faster onset of action and improved bioavailability. This is particularly beneficial for drugs with low aqueous solubility, which often exhibit poor absorption and erratic pharmacokinetic profiles. [22]

Bioavailability enhancement

- Improved absorption: CDs facilitate the absorption of drugs across biological membranes by maintaining a concentration gradient favoring drug diffusion. This leads to enhanced systemic exposure and therapeutic efficacy of the encapsulated drug molecules. [22]

- Protection of labile compounds: Labile drugs prone to degradation or metabolism can be encapsulated within cyclodextrin complexes, thereby protecting them from enzymatic degradation and first-pass metabolism. This preservation of drug integrity enhances bioavailability and ensures consistent pharmacological effects. [23]

Controlled drug delivery

- Sustained release formulations: Cyclodextrins enable the development of controlled release formulations by modulating the release kinetics of encapsulated drugs. By controlling factors such as CD/drug ratio and polymer crosslinking density, sustained drug release profiles can be achieved, leading to prolonged therapeutic effects and reduced dosing frequency. [24]

- Targeted drug delivery: CDs can be functionalized or conjugated with targeting ligands to achieve site-specific drug delivery. This targeted approach minimizes off-target effects, reduces systemic toxicity, and improves the therapeutic index of drugs, particularly in the treatment of localized diseases or tumors. [25]

Stability enhancement

- Prevention of drug degradation: CDs stabilize labile drug compounds by shielding them from environmental factors such as light, oxygen, and pH fluctuations. This stabilization prolongs the shelf life of pharmaceutical formulations and ensures consistent drug potency over time. [26]

- Masking of undesirable odors or flavors: Some drugs exhibit unpleasant odors or flavors, which can affect patient compliance. CDs can mask these undesirable attributes by encapsulating the aromatic molecules responsible for the off-putting sensory characteristics, thereby enhancing patient acceptability of the drug products. [27]

Formulation flexibility

- Versatile formulation options: Cyclodextrins offer formulation flexibility, allowing for the development of various dosage forms such as tablets, capsules, solutions, suspensions, and creams. This versatility enables pharmaceutical manufacturers to tailor formulations to meet specific patient needs and preferences. [28]

- Compatibility with excipients: CDs exhibit excellent compatibility with a wide range of excipients commonly used in pharmaceutical formulations. This compatibility simplifies the formulation process and ensures the stability and efficacy of the final drug product. [26]

Overcoming formulation challenges

- Rescue of failed formulations: CDs can salvage formulations of poorly soluble drugs that have failed during development due to solubility issues. By incorporating CDs into the formulation, drug candidates previously deemed unsuitable for further development can be re-evaluated and potentially brought to market. [29]

- Enhanced formulation stability: CDs stabilize formulation components such as emulsions, suspensions, and lipid-based delivery systems by reducing particle aggregation, preventing phase separation, and improving physical stability. This ensures the integrity and uniformity of the formulation throughout its shelf life. [29]

In summary, cyclodextrins are indispensable tools in pharmaceutical formulation and drug delivery, offering a wide array of benefits ranging from solubility enhancement to targeted drug delivery. Their versatility, compatibility, and ability to overcome formulation challenges make them invaluable assets in the development of safe, effective, and patient-friendly pharmaceutical products. Continued research and innovation in cyclodextrin-based drug delivery systems are expected to further expand their applications and impact in the pharmaceutical industry.

1-4. Advances in cyclodextrin polymers and cyclodextrin-based nanoparticles (CDNPs)

Recent advancements in cyclodextrin polymers have paved the way for innovative drug delivery systems with enhanced properties and functionalities. By refining synthesis techniques, researchers have achieved precise control over the characteristics of cyclodextrin polymers, including molecular weight, crosslinking density, and morphology. This optimization process, often involving direct polymerization of cyclodextrins with crosslinking agents such as epichlorohydrin, has yielded polymers tailored to specific application needs. Moreover, efforts to functionalize cyclodextrin polymers with targeting ligands, stimuli-responsive moieties, or imaging agents have expanded their capabilities, enabling the design of smart drug delivery systems capable of site-specific targeting and triggered release. These modifications not only enhance therapeutic efficacy but also enable real-time monitoring of drug delivery processes. Additionally, advancements in improving the biodegradability and biocompatibility of cyclodextrin polymers have addressed concerns regarding their safety profile, ensuring compatibility with biological systems and minimizing potential adverse effects. [30]

In parallel, significant progress has been made in the synthesis and optimization of cyclodextrin-based nanoparticles (CDNPs), leveraging novel techniques to precisely control their size, morphology, and surface properties. These advancements have expanded the therapeutic potential of CDNPs, particularly in targeted drug delivery and personalized medicine. Efforts to enhance drug encapsulation efficiency through strategies such as covalent conjugation, physical entrapment, and inclusion complexation have optimized drug loading capacity and release kinetics, improving therapeutic outcomes. Furthermore, advancements in stabilizing agents and surface modifications have bolstered the stability and drug release kinetics of CDNPs, enabling controlled release in response to specific triggers such as pH, temperature, or enzymatic activity. These innovations have propelled CDNPs to the forefront of drug delivery technology, offering versatile solutions to complex therapeutic challenges. [31]

Within this landscape, βCD crosslinked with epichlorohydrin (ECH) has emerged as a promising platform for the development of cyclodextrin-based nanoparticles (CDNPs) with enhanced properties and performance. Leveraging the hydrophobic interior cavity of βCD and the structural stability conferred by crosslinking with ECH, βCD-ECH-based CDNPs exhibit superior drug encapsulation efficiency compared to native cyclodextrins. [32, 33] Furthermore, these nanoparticles demonstrate excellent biocompatibility and safety profiles, positioning them as promising candidates for biomedical applications. Extensive research efforts have explored their therapeutic applications, ranging from cancer therapy to central nervous system drug delivery and treatment of inflammatory diseases. The versatility of βCD-ECH-based CDNPs in encapsulating a wide range of therapeutic agents and targeting specific tissues or cells holds great promise for advancing drug delivery technology and improving patient outcomes. Collectively, these advancements underscore the transformative potential of cyclodextrin-based materials in revolutionizing drug delivery and therapeutic interventions.

1-5. Significant of understanding binding constants and challenges in binding studies

Understanding the binding interactions between cyclodextrins (CDs) and guest molecules is crucial for designing effective drug delivery systems and optimizing therapeutic outcomes. Binding constants, which quantify the strength of these interactions, provide valuable insights into the stability and efficacy of CD-guest complexes. [34] However, determining binding constants accurately poses several challenges, necessitating the use of sophisticated analytical techniques and methodologies. Here, we discuss the significance of binding constants, common analytical techniques employed in binding studies, and the challenges associated with their determination.

Binding constants quantify the strength of molecular interactions between cyclodextrins and guest molecules, providing essential information about the stability and thermodynamics of CD-guest complexes. These constants dictate

the equilibrium between free and bound states, influencing crucial parameters such as drug solubility, release kinetics, and bioavailability. By elucidating the binding affinity of cyclodextrins for specific guest molecules, binding constants guide the design of drug delivery systems tailored to optimize drug loading, release profiles, and targeting efficiency.

Analytical techniques for determining binding constants encompass a range of methods tailored to quantify the strength of molecular interactions between cyclodextrins and guest molecules. The phase solubility method, a widely used approach, measures the solubility of the guest molecule in the presence of cyclodextrins to determine binding constants based on the increase in solubility upon complex formation. Titration methods, on the other hand, involve gradually adding one component to a solution containing the cyclodextrin while monitoring a physical property sensitive to the interaction, such as heat flow, NMR signal, UV absorption, or fluorescence intensity. These methods provide detailed insights into the binding process and allow for the determination of binding constants with high precision. Additionally, diffusion-ordered NMR spectroscopy (DOSY-NMR) offers a powerful tool for investigating molecular interactions and quantifying binding constants in complex mixtures. By measuring the diffusion coefficients of free and bound species, DOSY-NMR provides a direct method for determining binding constants without the need for chromophores or labeling, offering advantages such as non-destructive measurements and real-time monitoring of binding processes. Collectively, these analytical techniques facilitate the elucidation of host-guest interactions and provide valuable information for the design and optimization of cyclodextrin-based drug delivery systems.

One significant challenge in determining binding constants using methods other than DOSY-NMR is the inherent complexity of the binding process. Traditional techniques such as the phase solubility method and titration methods rely on indirect measurements of the binding interaction, which can introduce uncertainties and limitations. For example, the phase solubility method may

suffer from inaccuracies due to the presence of small aggregates and difficulties in determining the saturated concentration of organic compounds accurately. Similarly, titration methods require careful monitoring of physical properties such as heat flow, UV absorption, or fluorescence intensity, which may be influenced by experimental conditions and sample characteristics. These challenges can affect the reliability and accuracy of binding constant determinations, especially for complex systems involving multiple binding sites or dynamic equilibria.

Another challenge is the limited sensitivity and detection limits of traditional analytical techniques compared to DOSY-NMR. Techniques such as UV absorption or fluorescence spectroscopy may have higher detection limits, making it challenging to accurately quantify binding interactions for low-concentration compounds or weakly binding complexes. Moreover, these methods may lack the specificity to differentiate between free and bound species accurately, particularly in complex mixtures. As a result, determining precise binding constants using traditional techniques may require extensive optimization of experimental parameters and sample preparation methods to enhance sensitivity and minimize interference from background signals.

Additionally, data analysis and interpretation pose significant challenges in traditional binding studies, particularly when dealing with complex binding equilibria or overlapping signals. Extracting meaningful information from titration curves or solubility measurements requires sophisticated mathematical modeling and curve-fitting algorithms, which may introduce uncertainties and errors. Moreover, the interpretation of binding constants obtained from traditional techniques may be influenced by assumptions and simplifications made during data analysis, potentially leading to discrepancies between experimental results and actual binding behavior. Overcoming these challenges requires careful experimental design, validation, and verification using complementary techniques to ensure the accuracy and reliability of binding constant determinations.

In summary, diffusion-ordered NMR spectroscopy (DOSY) stands out as a valuable tool for determining the binding constants of cyclodextrin-based nanoparticles (CDNPs). DOSY offers several advantages, including non-destructive measurements, real-time monitoring of binding processes, and the ability to quantify binding constants without the need for chromophores or labeling. By measuring the diffusion coefficients of free and bound species, DOSY provides direct and accurate insights into host-guest interactions, facilitating the optimization of CDNPs for drug delivery applications. Overall, DOSY emerges as a powerful analytical technique for elucidating the binding behavior of CDNPs and advancing their therapeutic potential.

1-6. Nuclear magnetic resonance (NMR) spectroscopy in host-guest studies

Nuclear magnetic resonance (NMR) spectroscopy is a powerful analytical technique widely used in host-guest studies to elucidate the structural and dynamic properties of molecular complexes formed between a host molecule and a guest molecule. Host-guest chemistry involves the encapsulation of a guest molecule within the cavity or binding site of a host molecule through non-covalent interactions such as hydrogen bonding, van der Waals forces, π-π interactions, and hydrophobic effects. [35]

One of the key advantages of NMR spectroscopy in host-guest studies is its ability to provide detailed information about the molecular structure, stoichiometry, binding affinity, and dynamics of the complex in solution under physiological conditions. By recording one-dimensional (1D) and two-dimensional (2D) NMR spectra, researchers can analyze chemical shifts, coupling constants, relaxation rates, and NOE (nuclear Overhauser effect) interactions to characterize the host-guest complex.

Chemical shift perturbations (CSPs) in the NMR spectra of the host and guest molecules upon complex formation are often used to identify the binding sites and monitor the strength of interactions between them. Additionally, NOE measurements can provide distance constraints between protons within the complex, aiding in the determination of its three-dimensional structure. [36]

Furthermore, NMR spectroscopy can be employed to investigate the dynamics of host-guest complexes, including the rates of association and dissociation, conformational exchange processes, and ligand-induced conformational changes. Techniques such as relaxation dispersion NMR and exchange spectroscopy enable the characterization of transient or low-populated states within the complex, shedding light on dynamic binding mechanisms. [37]

In recent years, NMR spectroscopy has been extensively utilized in the study of various host-guest systems, including cyclodextrin complexes, cucurbiturils, calixarenes, and metal-organic frameworks (MOFs), among others. [38, 39] These

studies have contributed to our understanding of molecular recognition, supramolecular chemistry, drug delivery, catalysis, and materials science.

Overall, NMR spectroscopy plays a crucial role in host-guest studies by providing detailed structural and dynamic information about molecular complexes, thereby facilitating the design and optimization of novel host molecules for diverse applications in chemistry and biomedicine.

1-7. Diffusion-ordered NMR spectroscopy (DOSY) in determining the binding constant

Diffusion-ordered NMR spectroscopy (DOSY) has emerged as a valuable tool in the realm of host-guest chemistry, offering unique insights into molecular interactions and the formation of complexes in solution. [40] DOSY enables the differentiation of species based on their diffusion rates, making it particularly useful for studying host-guest systems where various molecular species coexist.

In host-guest studies, DOSY can provide several critical pieces of information:

1. Identification of Components: DOSY can distinguish between different molecular species present in solution, such as free host, free guest, and host-guest complexes. Each component typically exhibits a distinct diffusion coefficient, allowing for their identification based on the DOSY spectrum.

2. Characterization of Host-Guest Complexes: DOSY can elucidate the formation of host-guest complexes by observing changes in diffusion coefficients upon complexation. The diffusion coefficient of the host-guest complex is often slower compared to that of free host or free guest molecules due to their larger size and altered hydrodynamic properties.

3. Determination of Stoichiometry: By analyzing the DOSY spectrum, one can deduce the stoichiometry of the host-guest complex. The presence of multiple species with distinct diffusion coefficients may indicate the formation of complexes with different stoichiometries.

4. Quantification of Binding Affinity: DOSY can also be used to estimate the binding affinity between the host and guest molecules. Changes in the diffusion coefficient of the host molecule upon complexation can be correlated with the concentration of the guest molecule, providing insights into the strength of the host-guest interaction.

To apply DOSY in host-guest studies effectively, experimental parameters such as gradient strength, diffusion delay, and spectral acquisition parameters need to be optimized. Additionally, data analysis techniques, including curve fitting and

mathematical modeling, are employed to extract quantitative information from DOSY spectra.

In a host-guest system, DOSY can be used to distinguish between free host, free guest, and host-guest complex based on their respective diffusion coefficients. Typically, larger molecules such as host-guest complexes diffuse more slowly compared to smaller molecules like free host or free guest molecules. By analyzing the DOSY spectrum, it is possible to observe distinct diffusion profiles corresponding to each component of the system.

To determine the binding constant (K) of the host-guest complex, DOSY experiments are often conducted at various concentrations of the guest molecule while keeping the concentration of the host molecule constant. The binding constant can be extracted from DOSY data by analyzing the changes in the diffusion coefficient of the host molecule upon complexation with the guest molecule. The diffusion coefficient of the host-guest complex decreases due to the formation of larger species with slower diffusion rates.

Determining the binding constant (K) from DOSY experiments in a 1:1 host-guest complexation system involves a detailed series of steps. Initially, the equilibrium concentrations of the host ([H]), guest ([G]), and complex ([HG]) are established. This involves accounting for their initial concentrations $[H]_i$ and $[G]_i$ and the formation of the complex, as described by the equilibrium relationship $[H]_i = [H] + [HG]$ and $[G]_i = [G] + [HG]$. These relationships allow for the determination of the molar fractions of free host and guest molecules, denoted as f_H and f_G , respectively. These fractions are calculated based on the differences between the initial and equilibrium concentrations of the species. When the molecular exchange between complexed and uncomplexed states occurs much faster than the NMR timescale, the observed diffusion coefficient represents the molar fraction weighted average of the diffusion properties of these two states[41]:

$$D_{\mathrm{H}}^{*} = f_{\mathrm{H}} D_{\mathrm{H}} + \left(1 - f_{\mathrm{H}}\right) D_{\mathrm{HG}}$$
$$\vdots$$
$$D_{\mathrm{G}}^{*} = f_{\mathrm{G}} D_{\mathrm{G}} + \left(1 - f_{\mathrm{G}}\right) D_{\mathrm{HG}} \quad (1)$$

Here, D_{H}^{*} and D_{G}^{*} are the observed diffusion coefficients of host and guest in their mixtures.

By solving a simultaneous equation derived from the DOSY experiment, which relates the observed diffusion coefficients to the known diffusion coefficients and molar fractions, the diffusion coefficient of the host-guest complex. D_{HG} and the concentration of the complex ([HG]) can be obtained.

Finally, utilizing these values, the binding constant (K) is calculated using the equation:

$$K = \frac{[\mathrm{HG}]}{[\mathrm{H}][\mathrm{G}]} \quad (2)$$

This binding constant provides quantitative insight into the strength of the host-guest interaction, offering valuable information for understanding molecular recognition processes and optimizing the design of host-guest systems for various applications.

Overall, DOSY serves as a valuable tool for investigating host-guest interactions, providing crucial information about complex formation, stoichiometry, and binding affinity in solution. Its application in host-guest studies complements other analytical techniques, contributing to a comprehensive understanding of supramolecular chemistry and molecular recognition processes. DOSY is a powerful NMR technique providing valuable information about the diffusion coefficients of different species in solution, allowing the differentiation of molecules based on their size, shape, and interactions. DOSY spectroscopy is a valuable tool in host-guest studies for characterizing molecular complexes and determining binding constants, allowing researchers to gain insight into the nature of host-guest interactions and optimize the design of supramolecular systems for various applications.

1-8. Previous studies and objectives

Our previous studies synthesized CDNPs using βCD and ECH, optimizing their particle size and CD content to enhance drug loading and binding constants. Notably, α-mangostin (MGS), a hydrophobic xanthone derivative with anticancer properties, showed significantly increased binding and loading ratios when encapsulated in CDNPs compared to native CDs.

This thesis delves into the intricacies of inclusion complexes formed by cyclodextrin-based nanoparticles (CDNPs) with vanillin and paroxetine hydrochloride hemihydrate (PRX), a hydrophobic antidepressant drug. Leveraging advanced analytical techniques, particularly diffusion-ordered NMR spectroscopy (DOSY-NMR) alongside other methods, this study sets out to achieve several objectives:

1. Determining binding constants: The primary objective is to quantify the binding constants between CDNPs with vannilin and PRX accurately. By employing DOSY-NMR and complementary analytical approaches, the study seeks to elucidate the strength and thermodynamic parameters of the interactions between CDNPs and PRX, shedding light on the efficacy of CDNPs as drug carriers.

2. Exploring molecular mechanisms: Another aim is to delve into the molecular mechanisms underlying the interactions between CDNPs with vanillin and PRX. Through detailed analysis of DOSY-NMR spectra and other techniques, the study endeavors to unravel the structural features and binding modes driving the formation of CDNP-drug complexes, offering insights into their stability and functionality.

3. Comparing effectiveness: Additionally, the study aims to compare the effectiveness of CDNPs with native cyclodextrins in enhancing drug solubility and stability. By assessing the solubilization efficiency and binding affinities of CDNPs versus free cyclodextrins, the research aims to delineate the advantages of nanoparticle-based drug delivery systems over conventional cyclodextrin formulations.

4. Assessing biotoxicity: Lastly, the thesis seeks to evaluate the biotoxicity of βCDNPs and determine their potential safety profile. The study aims to comprehensively assess the biocompatibility and toxicity of βCDNPs, crucial for their translational potential in pharmaceutical applications.

By addressing these objectives, this thesis aims to contribute to a deeper understanding of CDNP-drug interactions, their potential as drug delivery systems, and their safety profile, thereby advancing their development and application in biomedicine.

Chapter 2. Dramatically increased binding constant of cyclodextrin nanoparticles with vanillin exploring with diffusion ordered NMR spectroscopy (DOSY)

2-1. Introduction

Cyclodextrins (CDs) are cyclic oligosaccharides composed of α-1,4-linked glucoses that are produced in the enzymatic treatment of starch.[42] CDs exist in nature, albeit in minute amounts, and are found in various fermented products, including beer and bread. Among them, three types of CDs are synthesized at a large scale and commercially available, which are six- (αCD), seven- (βCD), and eight-membered rings (γCD). Application of CDs have been established in various fields including pharmacy, food, chromatography, catalysis, agriculture, cosmetics, medicine, and textiles.[43-45] CDs are now attracting significant attention as key materials for environmental chemistry.[46] They have a hydrophilic outer surface and a hydrophobic central cavity, providing the ability to form complexes with many hydrophobic compounds; as a result, these hydrophobic compounds can be dispersed in water as a complex with CDs, providing various physicochemical advantages, including stability and bioavailability. This is the main reason for the broad application of CDs.[43] This remarkable encapsulation is one of the most well-known and -studied "host-guest"-type supramolecular interactions. In the pharmaceutical field, CDs have been applied as solubilizers for hydrophobic drugs to increase bioavailability and to control pharmacokinetics.[45] CDs have become particularly indispensable in the formulation of steroids and prostanoid, which indeed has revolutionized anesthesia and obstetric medicine.[47]

Recently, numerous CD-containing polymers have been designed to control the particle size and the binding affinity of drugs.[48-50] The polymerization of CDs is carried out via a direct reaction between their hydroxyl groups and a coupling agent to form water-soluble or -insoluble polymers. Among them, epichlorohydrin (ECH) is considered as the most commonly used crosslinking agent. Its widespread use is due to its high reactivity with CDs, simple synthesis

reaction, and flexibility allowing various types of materials to be obtained, including hydrogels/gels, powders/particles, beads/resins, and nanoparticles/nanobeads.[51] For example, water-insoluble cyclodextrin polymers have been developed as materials for adsorbing organic pollutants such as methylene blue, bisphenol A, and metal ions.[52-58] In pharmaceutical applications, the water-soluble CDs polymers are of particular interest as a drug delivery system (DDS) given their ability to improve the solubility in aqueous solution as well as the bioavailability of some drugs beyond those with native CDs.[59-61] For example, the aqueous solubility of glipizide was reported to increase in the presence of the βCD-ECH polymer and the dissolution rate of glipizide from the β-CD-ECH polymer complex was significantly greater than that of the drug itself.[62] In general, a large binding constant ($> 10^4$ M^{-1}) between the DDS-carrier and the drug is required in order to maintain a stable complex and improve bioavailability after intravenous administration. However, it is rare to form a CDs complex with such a large binding constant. Recently, we synthesized various CD-ECH polymers (hereinafter referred to as CDNPs) with different CD contents, and found that CDNPs dramatically increased the binding constants of α-mangostin (MGS) to nearly 100 folds compared CDs themselves,[1] where MGS is a xanthone derivative and well known as an antioxidant and antigenotoxic agent. In these works, we measured the absolute weight-averaged molecular weight (M_w), hydrodynamic radius (R_h), and CD content and found how to control these physical characteristics by changing the reaction time, ECH/CD ratio, and pH of the polymerization solution. In some cases, the addition of amphiphilic molecules as a phase transfer catalyst is useful to control the properties.[63] We also investigated the inclusion complex with MGS as a potential anticancer drug[64] and an agent for removal of reactive oxygen species during ischemia-reperfusion (paper and patent in preparation), but the molecular mechanism of the inclusion of MGS by CDNPs still remains unclear. Although not for epichlorohydrin-linked CDs, Ma and Li found that the binding constant dramatically increased by about five orders of magnitude for diisocyanate-linked CDs by measuring UV absorbance.[65] As far as we know, this is the first paper to

report the dramatic enhancement of the binding due to the polymerization of CDs. Before the work of Ma and Li, there are several papers in which the water solubility of hydrophobic molecules is considerably improved by the polymerization of CDs. However, they did not observe a dramatic increase of binding constant.[66, 67] Karoyo and Wilson claimed that the results of Ma and Li may be due to an artifact resulting from the presence of an additional binding site created at the outside of CD or the linker molecule.[68] It appears that, within the field of cyclodextrin chemistry, no definitive conclusions can yet be drawn about the increased binding of CD polymers and their molecular mechanism.

Numerous analytical methods are available for the accurate determination of the binding constant of the inclusion complexes made from CDs and guests.[69] The most commonly used and easiest approaches are the phase solubility and titration methods.[70] In the solubility method, the solubility of the guest is measured after mixing CD and the guest molecule, and the binding constant is determined from the increment of the solubility from that of the solution saturated with the guest molecule alone. The phase solubility method is useful and convenient. However, the accuracy of the binding constant is strongly affected by the presence of small aggregates dispersed in water, which is sometimes difficult to distinguish from solubilized molecules. In fact, it is difficult to determine the saturated concentration of some organic compounds accurately. Generally, in the case of low intrinsic solubility, the error of the binding constant becomes large.[70] In the titration method, one component (usually the guest) is gradually added to the solution containing the host while monitoring a physical property such as heat flow, specific chemical resonance (in NMR), absorption band (in UV), or fluorescence intensity that is sensitive to the interaction of interest.[71] Recently, diffusion-ordered NMR spectroscopy (DOSY–NMR) has been developed and provides a new additional NMR-based method and an alternative method to investigate the binding constant between CDs and guest molecules.[41] An interesting feature of this technique is that the binding constant can be derived from the diffusion coefficient. In a fast exchange process between free and bound states of the component, its observed diffusion coefficient represents population

weight average of the diffusion properties of these two states.[41] Therefore, the fraction of each component can be evaluated from DOSY and thus the binding constant can be determined. Advances in NMR spectroscopy and computing have made high-resolution DOSY more readily available. High-resolution DOSY can distinguish small differences of about 1% in diffusion coefficient and overlapping signals coming from two different objects that differ in diffusion coefficient by at least 30% can be distinguished.[72] Furthermore, NMR does not require a chromophore for either the host or the guest and can provide molecular information on the binding model. Recently, DOSY has been applied to study the binding behavior of the inclusion complexes of CDs, but there has been no work to investigate CD-based polymers by use of DOSY.[73, 74]

This chapter investigates the inclusion complexes of CDNPs with vanillin (4-hydroxy-3-methoxy benzaldehyde, see Figure 2-1A for its chemical structure) as a representative guest molecule, compared with CDs themselves. Vanillin was chosen instead of MGS because the solubility of vanillin in water is quite suitable for NMR experiments, whereas that of MGS is too small to allow accurate NMR experiments. Additionally, the interaction between vanillin and CDs has been studied by various groups and it is now well-established that (1) vanillin forms a stable 1:1 complex with βCD,[75-77] (2) the binding constant between them in water at ambient temperate ranges from 10 to $2 \times 10^2\ M^{-1}$, depending on the method and reseachers[73, 76, 77] and (3) vanillin is oriented with the phenolic end nearer to the narrower end (or lower rim) and the aldehyde end near to the wider end (upper rim) of βCD.[77] By use of such well-studied vanillin, we should be able to clarify the molecular mechanism of the CDNP–vanillin interaction by two-dimensional (2D) ROESY and NOESY and examine the binding constant for various types of CDNPs using DOSY.

2-2. Experimental

2-2-1. Materials

Vanillin (catalog number 44020–30, purity > 98%) was supplied by Kanto Chemical Co., Inc. (Tokyo, Japan), and used without further purification. α-, β-, and γ-cyclodextrins and ECH (purity > 99%) were purchased from Tokyo Chemical Industry Co. (Tokyo, Japan), and used without further purification. Deuterium oxide (99.8%) was obtained from Fujifilm Wako Pure Chemical Co. (Osaka, Japan). We compared the inclusion phenomena between vanillin and its analogs: homovanillic acid (HVA) and vanillyl mandelic acid (VMA); both of these latter compounds were supplied by Tokyo Chemical Industry Co. (Tokyo, Japan; purity > 98%) and used without further purification. All other chemicals and solvents were of commercial grade and used as received.

2-2-2. Preparation and characterization of CDNPs

Four types of βCDNP with different ECH/CD weight ratios were prepared by changing the ECH feeding amount, as shown in Table 1. This polymerization reaction is a nucleophilic addition reaction of hydroxyl groups under basic conditions, the details of which are described elsewhere.[33] The obtained solution was purified by dialysis for 2 days using a membrane (molecular weight cut-off, 3500). During the dialysis, water-undissolved components were precipitated, and we used the supernatant that contains CDNP. Occasionally, we filtered the solution to remove large particles. The weight-averaged molecular weight (M_w) was determined by static light scattering coupled with gel-chromatography. The hydrodynamic radius (R_h) was determined by dynamic light scattering. The detailed procedures of these scattering experiments are described in our previous paper[33] as well as in the Appendix A. The CD content in CDNPs was determined by the phenol sulfuric acid method.[78] As a negative control of CDNPs, we prepared an ECH polymer from dextran (M_w = 40 kDa; denoted DXNP), whose molecular characteristics are also listed in Table 1. The inclusion phenomena of βCDNPs and HVA or VMA were also studied in a similar manner as for vanillin.

2-2-3. NMR measurements

All NMR experiments were performed on a JEOL JNM-ECZ500R spectrometer operating at 500 MHz with a stationary magnetic field of strength 11.74 T at the analytical center of the University of Kitakyushu. All tested solutions were prepared 1 day before the measurements to ensure complete solubilization. In the ^{1}H NMR experiment, the concentrations of vanillin and CDs were all set to 10 mM. For the case of CDNP, the concentration of CDNPs was set so as the CD concentration was 10 mM. Two-dimensional nuclear overhauser effect spectroscopy (NOESY) and rotating frame overhauser effect spectroscopy (ROESY) experiments were performed to characterize the structure of βCD and $\beta CDNP_{0.9}$ complexes formed with vanillin, respectively. ROESY and NOESY NMR spectra were acquired using a standard pulse sequence from the JEOL library at 25 °C. The relaxation delay between successive pulse cycles was 3.9 s for βCD-Val ROESY and 2.5 s for $\beta CDNP_{0.9}$-Val NOESY. Mixing times of 0.3 s and 1.9 s were used for ROESY and NOESY, respectively.

Diffusion coefficients were obtained through DOSY experiments using a BPP longitudinal eddy current delay (BPP-LED) sequence at 20 ± 0.5 °C in 5 mm tubes. The duration of the magnetic field pulse gradients δ was 3 to 4 ms, depending on the sample. The pulse gradient strength was increased from 30 to 300 T/m. The diffusion times were optimized between 0.1 s for vanillin and 0.15 s to 0.4 s for each host sample to completely decrease the signals by a factor of 10–20 and better analyze the exponential signal decay. After measurement, the DOSY experimental data were processed using the software Delta 5.3 (JEOL Ltd.,Tokyo Japan). After baseline correction, phase correction, and Fourier transformation, the diffusion coefficients were obtained from the peak intensity $I(G_z)$ and exponential fitting to satisfy the Stejskal-Tanner equation[79]:

$$I(G_z) = I(0)\exp\left[-D(\gamma\delta G_z)^2\left(\Delta - \frac{\delta}{3}\right)\right] \quad (3)$$

where $I(G_z)$ is the NMR spectral intensity at a gradient with strength G_z, $I(0)$ is the spectral intensity at zero gradient in Gauss/cm units γ is the gyromagnetic ratio, Δ is the time interval between the first and second gradient pulses, and D is the translational diffusion coefficient. The D value for the given solution was

obtained by taking the average of the diffusion coefficients of several different protons. To display the data two-dimensionally, the inverse Laplace transformation of the Y-axis was performed on every point of data that was Fourier-transformed along the X-axis. The translational diffusion coefficient is related to the hydrodynamic radius (R_h) by the following Stokes-Einstein equation:

$$D = \frac{k_B T}{6\pi\eta R_H} \tag{4}$$

where k_B is the Boltzmann constant, T is the absolute temperature, and η is the viscosity of the medium (in the present experiment, we used η = 1.2467 mPa·s). Dynamic light scattering also provides D, although its accuracy is not as good as DOSY. We compared the R_h values obtained by these two methods.

2-2-4. Estimating the binding constant from DOSY experiment

Same as described in Chapter 1, Section 1-7.

2-2-5. Job plot to determine the stoichiometry

We determined the stoichiometry of the complexation between βCDNP and vanillin by the continuous variation method (Job plot) with NMR (for details, see the Appendix A). We chose the H-5 proton of vanillin because it was most affected by the complex formation. A series of vanillin/βCDNP solutions were prepared by varying the molar fraction of the vanillin within the range of 0–1. The stock concentration of both vanillin and βCDNP were 4.9 mM. Here, the concentration of βCDNP is calculated based on the βCD units in βCDNP. All of the ^{1}H-NMR measurements were performed at 25 °C.

2-3. Results and discussion

2-3-1. CDNPs and their characteristics

Table 1 shows all samples used in this experiment; some of them were newly synthesized and the others were the same as in the previous works.[33] We synthesized a dextran-based ECH hyperbranched polymer as a comparison material (denoted by DXNP). In the sample codes of CDNPs, the prefix and suffix indicate the type of CD and the ECH/CD weight ratio in the polymer, respectively. Typical examples of a gel permeation chromatography coupled with multi angle light scattering (GPC-MALS) chromatogram and the angular dependence of static light scattering to determine M_w are shown in the Appendix A. The obtained values of the average molecular weight (M_w) are summarized in the third column. The angular dependence of the excess Rayleigh ratio was too small to obtain reliable values on the radius of gyration, so it is not shown. The fourth and fifth columns show the hydrodynamic radius (R_h) determined by dynamic light scattering and DOSY, respectively. As shown in the Appendix A, the distribution of R_h was unimodal because we removed small particles by dialysis. The weight percent of CDs was determined by the phenol sulfuric acid method[78] and converted into the number of CDs in one CDNPs particle (N_{CD}) using M_w. As we reported already, N_{CD} decreased with an increase of the ECH ratio, but the particle sizes remained less than 10 nm. The weight ratios of ECD to CDs in CDNPs were calculated from the weight percent of CDs and M_w. We confirmed that the phenol sulfuric acid method could determine the weight percent of CDs within ±5% and that the ECH polymer without CD showed 0% of carbohydrates by use of this method.

We obtained ^{1}H-NMR spectra of $\beta CDNP_{0.9}$ in DMSO and the results showed the disappearance of all -OH peaks as shown in Figure A1. $\beta CDNP_{0.9}$ had the lowest ECH ratio and even this sample showed no sugar hydroxyl protons, suggesting that most of the hydroxyl groups of CDs had reacted with ECH.

Table 2-1. Sample lists used in this work, including the molecular characteristics determined by GPC-MALS and the phenol sulfuric acid method. Feeding weight ratio is the weight ratio between ECH and CD in the synthesize reaction. ECH/CD in polymer is weight ratio between ECH and CD in the polymer.

Sample code	Feeding weight ratio	M_w (g/mol) [a]	R_h (nm) [b]	R_h (nm) [c]	N_{CD} [d]	*wt%* CD (%)	ECH/CD in polymer (w/w)
$\beta CDNP_{0.9}$	2.83	9.37×10^4	4.0	5.6 ± 0.1	43.8	53.0	0.9
$\beta CDNP_{2.0}$	4.25	2.74×10^5	7.1	8.8 ± 0.2	79.4	32.9	2.0
$\beta CDNP_{2.7}$	4.25	7.29×10^4	3.5	3.9 ± 0.2	17.1	26.7	2.7
$\beta CDNP_{3.0}$	5.66	1.55×10^5	5.6	8.0 ± 0.5	34.3	25.1	3.0
$\alpha CDNP_{3.2}$	4.25	2.43×10^4	2.1	2.6 ± 0.2	5.9	23.8	3.2
$\gamma CDNP_{3.3}$	4.25	1.23×10^5	4.0	6.6 ± 1.0	21.9	23.2	3.3
DXNP	2.83	1.98×10^5	3.8	-	-	-	-

a) Determined by GPC coupled with SLS, the estimated error range is about ±3 –±5%

b) Determined with DLS

c) Determined with DOSY

d) From the phenol sulfuric acid method, the estimated error range is about ±5%.

2-3-2. 1D and 2D 1H NMR and the Stoichiometry of the complex

The ^{1}H-NMR spectra of vanillin, βCD, $\beta CDNP_{2.7}$, vanillin-βCD mixture, and vanillin-$\beta CDNP_{2.7}$ (βCD/vanillin molar ratio of 1:1 for both samples) in D_2O are shown in Figure 2-1. Ferrazza et al showed that, when the concentration of vanillin was increased, a significant upfield shift was observed for the positions of all proton peaks owing to the water-dispersing aggregates of vanillin. We confirmed no such shift in vanillin. The peak assignments of free vanillin and βCD are shown in 2-1C (the proton numberings are shown in Figure 2-1A and B). Referring to the free vanillin and previous work, we also assigned the vanillin peaks in βCD and $\beta CDNP_{2.7}$. The magnified peaks in this region are shown in Figure 2-1E. It is clear that the complexation with βCD and $\beta CDNP_{2.7}$ caused a downfield shift and no peak splitting was observed. In the mixtures, there are two types of vanillin, free and complexed states, and the absence of new splitting resonances indicates that the interconversion between the free and complexed

states is faster than the NMR timescale. The downfield shift due to the complexation with CD has been observed by other groups and can be ascribed

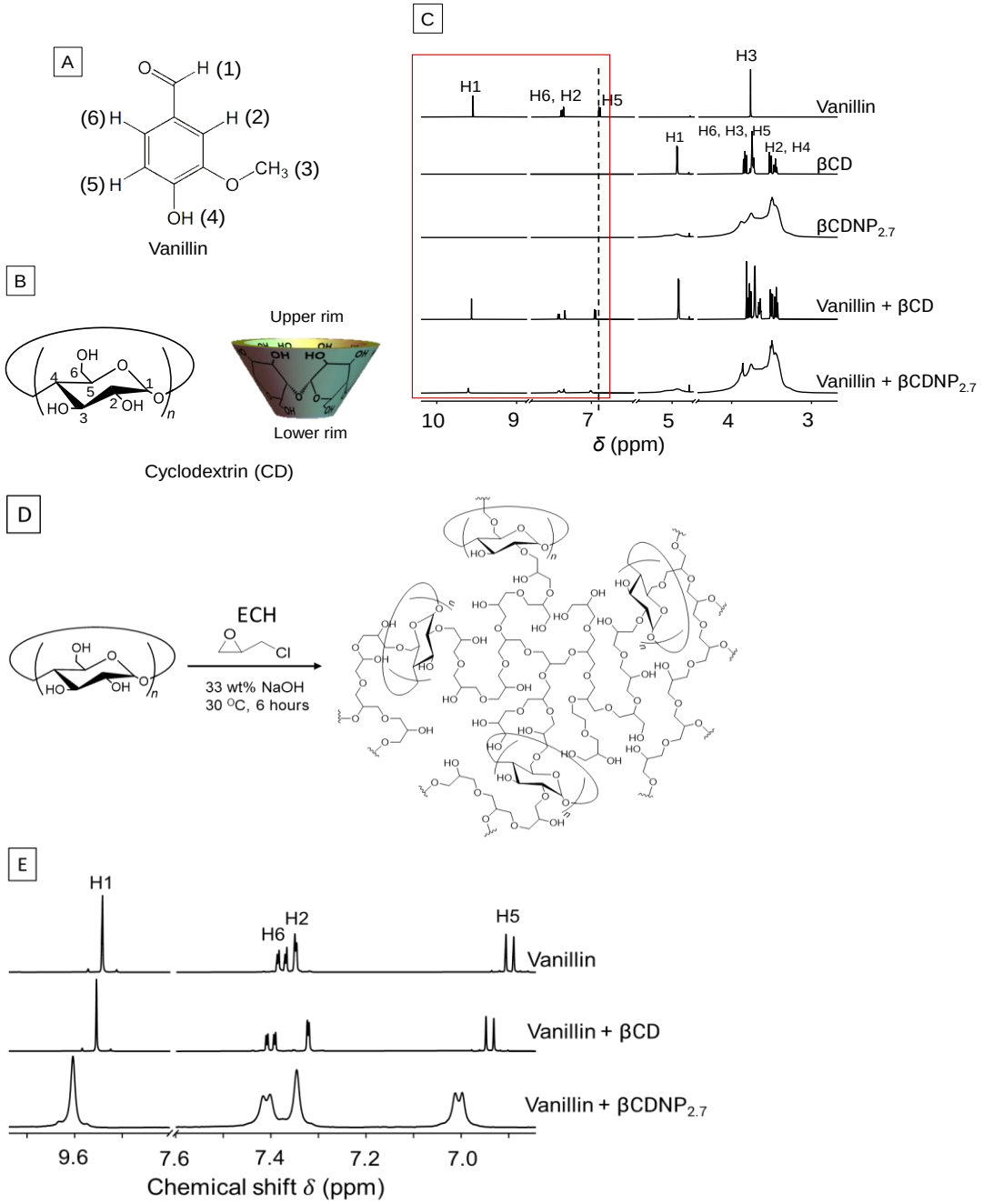

Figure 2-1. Chemical structures and proton numbers of vanillin and cyclodextrin (CDs) as well as the three-dimensional structure of CDs, and ^{1}H-NMR spectra of vanillin, βCD, $\beta CDNP_{2.7}$, vanillin-βCD and vanillin-$\beta CDNP_{2.7}$ mixtures. The intermediate δ regions of the spectra are enlarged in D. A: The chemical structure of vanillin. B: The chemical structure and three-dimensional structure of CDs. C: ^{1}H-NMR spectra of vanillin, βCD, $\beta CDNP_{2.7}$, vanillin-βCD and vanillin-$\beta CDNP_{2.7}$ mixtures. D: Synthesis scheme of cyclodextrin-based hyperbranched polymers (CDNPs) through polyaddition reactions with ECH. E: The intermediate δ regions 6.85 ppm to 9.75 ppm of the ^{1}H-NMR spectra of vanillin, vanillin-βCD and vanillin-$\beta CDNP_{2.7}$ mixtures.

to less shielding as a result of the lower-electron-density environment in the complexed state than in the free state. This type of downfield shift is normally observed in CD-inclusion complexes such as βCD-nicardipine hydrochloride, sodium picosulfate and D(−)-chloramphenicol.[80-82] The unexpected upfield shift of H-2 could be due to a conformational effect of the aldehyde C=O which should have a deshielding effect on the H-2 depending on its location.

Table 2 compares the chemical shifts (δ_{Val}) for five protons in vanillin among the three solutions: vanillin itself, vanillin in a mixture with βCD, and vanillin in a mixture with $\beta CDNP_{2.7}$. The differences between the vanillin alone and the mixtures are shown in the fourth and sixth columns denoted by $\delta_{Val/CD}$ and $\delta_{Val/CDNP}$, respectively. $\delta_{Val/CD}$ for H-5 and H-6 were 0.02–0.04 ppm, while those of H-1 and H-2 were lower. These features indicate that the H-5 and H-6 side of the aromatic ring digs more deeply into the CD cavity than the H-1 and H-2 side. The small change in H-1 suggests that the aldehyde group is most likely located at the upper rim or outside of the CD (as confirmed later by NOESY). This molecular arrangement is consistent with the previous work by Divakar.[83] In $\beta CDNP_{2.7}$-vanillin, H-5 showed a larger change in δ_{Val} than in βCD-vanillin. Even H-1 showed an appreciable change. These differences between βCD and βCDNP suggest that the binding mode is different between them. The larger δ_{Val} can be explained in two ways: the population of bound vanillin is increased and/or a less shielded environment is created. Based only on 1D ^{1}H-NMR, we cannot draw conclusions about which is more likely. H-6 and H-5 are neighboring protons and it seems difficult to understand why H-6 showed a small shift while H-1 and H-5 showed clear increase.

Table 2-2. Chemical shifts of four vanillin protons before and after mixing with CD or $\beta CDNP_{2.7}$

	δ_{Val}	δ_{Val} mixed with bCD	$\Delta\delta_{Val/CD}$	δ_{Val} mixed with $bCDNP_{2.7}$	$\Delta\delta_{Val/CDNP}$
H-5	6.907	6.949	0.042	7.013	0.106
H-2	7.347	7.324	−0.022	7.346	−0.001
H-6	7.388	7.411	0.023	7.416	0.028
H-1	9.543	9.555	0.013	9.604	0.061

The stoichiometric ratio of the complexation of βCD and vanillin has been studied by many groups and it is well established that they form a 1:1 complex.[84] To obtain the stoichiometric ratio between $\beta CDNP_{0.9}$ and vanillin, we constructed a Job plot from the H-5 proton chemical shift by changing the composition (Figure 2-2). Figure 2-2 plots $[G]_i\Delta\delta_G$ against r, where $[G]_i$ and $\Delta\delta_G$ are the total (free plus complexed) guest molecule concentration and the difference in chemical shifts of guest in the absence and presence of host for a given ratio r, and r is the composition ratio defined by $r = [G]_i/([G]_i + [H]_i)$ with $[H]_i$ being the βCD concentration of βCDNP in the solution. The total concentration of $[G]_i + [H]_i$ was kept constant at 4.9 mM. The $[G]_i\Delta\delta_G$ value peaked at $r = 0.5$, indicating 1:1 binding. Therefore, the data points were fitted by the following equation for this binding mode [85]:

$$\Delta\delta_G = \Delta\delta_{HG}\left(\frac{[HG]}{[G]_i}\right) = \frac{\Delta\delta_{HG}}{2[G]_i}\left[[H]_i + [G]_i + \frac{1}{K} - \sqrt{\left([H]_i + [G]_i + \frac{1}{K}\right)^2 + 4[H]_i[G]_i}\right] \quad (5)$$

Here, $\Delta\delta_{HG} = \delta_{HG} - \delta_G$ is the difference in chemical shifts of complex and guest in the absence of host. The data points were nicely fitted by the curve based on 1:1 binding and the best fitting gave the value of $K = 10^3\ M^{-1}$. Comparing with the fitted curve, which appears to show the maximum and minimum K values, the error range of this estimation is $K = (0.8–1.25) \times 10^3\ M^{-1}$. The obtained value is consistent with that from DOSY. We constructed a Job plot for βCD and vanillin and compared it with that of $\beta CDNP_{0.9}$ and vanillin, confirming that the K value is around 95 M^{-1} and there is 1:1 binding. To sum up the result of the

Job plot, the main binding mode between βCDNP$_{0.9}$ and vanillin is 1:1 complexation similarly to that of βCD and vanillin and the binding constant between βCDNP$_{0.9}$ and vanillin appeared to be much larger than that of βCD and vanillin.

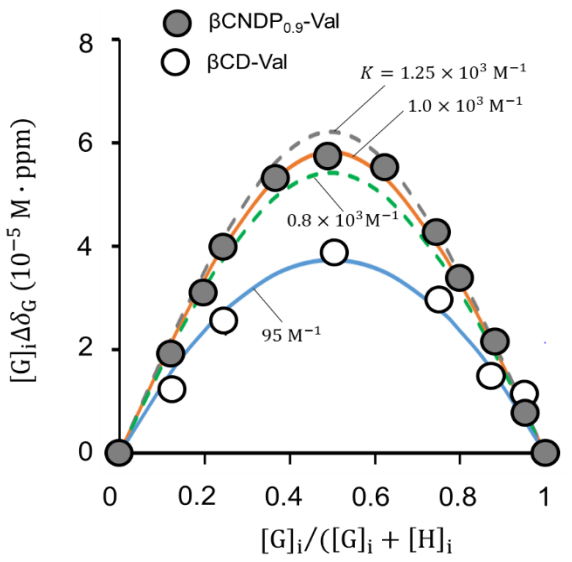

Figure 2-2. Job plots for vanillin and βCDNP$_{0.9}$ in D_2O at 25 °C, comparing with βCD. The total concentration $[G]_i + [H]_i$ was fixed at 4.9 mM. The dotted and solid lines are calculated from Eq 5 assuming K = 1.25×10^3, 1.0×10^3, 0.8×10^3 and 90 M^{-1} (from the top), respectively.

Figure 2-3 shows ROESY and NOESY 2D spectra for βCD-Val and βCDNP$_{0.9}$-Val, respectively. βCD-Val showed clear intermolecular dipolar interactions between the phenyl ring protons and the βCD cavity protons, while the correlation between H-1 of vanillin and βCD was too moderate to be observed. This suggests that the vanillin molecule has the phenol side inside the cavity and the aldehyde part outside it. This is consistent with the previous discussion as well as other studies.[76, 77] In contrast, βCDNP$_{0.9}$-Val shows the correlation between H-1 and βCD as well as all of the phenyl ring protons. This difference suggests that the vanillin molecule enters more deeply into the βCD cavity in βCDNP than in βCD, including the H-1 proton as shown by the inset model. This result is consistent with that of ^{1}H-NMR: appreciable change in $\Delta\delta_{Val/CDNP}$ was observed in βCDNP, while there was no remarkable change in CD. Note that we used two different 2D NMR methods. This is because NOESY is suitable for

small (M_w < 1000 Da) and large (M_w > 2000 Da) molecules for which nuclear overhauser effects are positive and negative, respectively, but may fail for medium sized molecules. This explains why the cross peaks of βCDNP-Val were successfully observed by NOESY, but no such dipolar interactions between βCD and vanillin were detected.[86] Therefore, ROESY was used as the technique of choice for medium-sized molecules to investigate βCD-Val.

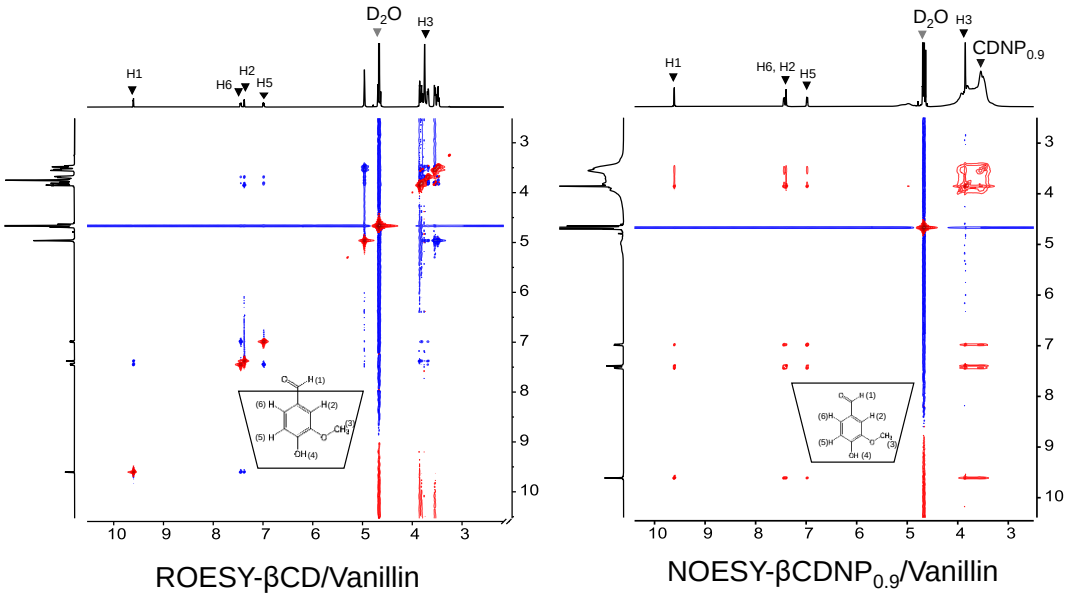

Figure 2-3. The 2D ROESY and NOESY spectra of βCD-Val and $βCDNP_{0.9}$-Val solutions at 25 °C: the molar ratio of vanillin:βCD was 1:1 and the concentrations of all of vanillin, βCD, and βCD in $βCDNP_{0.9}$ were 10 mM.

2-3-3. Determining the binding constant of CDNP–vanillin with DOSY-NMR

Figure 2-4 plots ln $I(0)/I(G_z)$ against $(\gamma\delta G_z)^2$ for the H-5 proton of vanillin of several samples. The diffusion coefficients (D) were determined from the slope and the binding constant K was determined using Eq 2. We carried out similar fitting as for H-5 shown in the figure for the other protons and the obtained values coincided within ±5%; an example of the obtained values for Val-$βCDNP_{2.7}$ is presented in the Appendix A. In some cases, the data points had a relatively large error as shown in Figure 2-4A. For such cases, the error range can be estimated as at most ±10%, which affected the final binding constant by ±21%. Table III

summarizes all the data including HVA and VMA: vanillin analogs are described later.

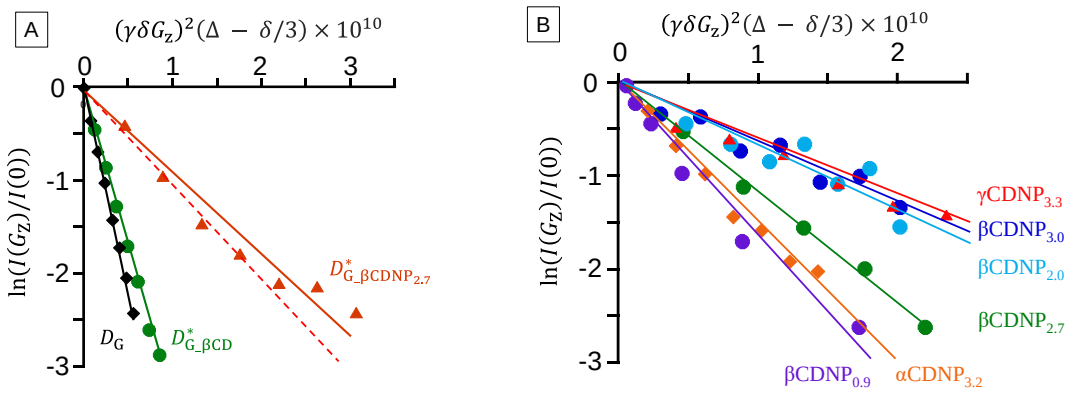

Figure 2-4. A: The signal intensity ratio ln $I(0)/I(G_z)$ plotted against the exponential term in Eq 3, where $I(G_z)$ is the signal intensity at the end of the spin-echo after applying the gradient intensity of G_z and $I(0)$ is the signal intensity at the end of the spin-echo in the absence of the gradient pulse. Here, the intensity of the H-5 proton of vanillin is plotted. The red-dotted line fitted to $\beta CDNP_{2.7}$ shows the upper limit of the estimated diffusion coefficient (D = 10^{-10} m^2/s, K = 4.4 × 10^3 M^{-1}), while the red-solid line shows the result fitted by the least-squares method (D = 9 × 10^{-11} m^2/s, K = 6.8 × 10^3 M^{-1}). B: The diffusion profile of the H-5 proton of vanillin in the mixture with different CDNPs samples.

Table 2-3. Obtained values of the diffusion coefficient of D^*_G in Eq 1 and determined K values for all samples.

Guest	Host	D^*_G (10^{-10} m^2/s)	K (M^{-1})
Val	αCD	4.01 ± 0.04	16
	βCD	3.77 ± 0.44	55
	γCD	3.47 ± 0.25	97
	$\beta CDNP_{0.9}$	1.54 ± 0.33	1.07 × 10^3
	$\beta CDNP_{2.0}$	0.78 ± 0.05	4.43 × 10^3
	$\beta CDNP_{2.7}$	0.90 ± 0.04	6.88 × 10^3
	$\beta CDNP_{3.0}$	0.68 ± 0.04	8.35 × 10^3
	$\alpha CDNP_{3.2}$	1.75 ± 0.16	0.93 × 10^3
	$\gamma CDNP_{3.3}$	0.67 ± 0.05	1.00 × 10^4
HVA	βCD	3.65 ± 0.40	0.13 × 10^3
	$\beta CDNP_{0.9}$	2.33 ± 0.07	0.48 × 10^3
	$\beta CDNP_{3.0}$	1.79 ± 0.08	1.20 × 10^3
VMA	βCD	3.78 ± 0.13	0.12 × 10^3
	$\beta CDNP_{0.9}$	2.13 ± 0.53	0.84 × 10^3
	$\beta CDNP_{3.0}$	1.63 ± 0.55	1.88 × 10^3

Based on the D values for each peak, we constructed a 2D DOSY plot in Figure 2-5 for βCD-vanillin and $\beta CDNP_{2.7}$-vanillin with a peak width determined by the estimated error of the diffusion coefficient obtained from the fitting process.

The vertical axis shows the chemical shift of ^{1}H NMR of the mixtures and the horizontal one is the obtained D value. The green and orange solid lines represent $D^*_G \equiv D^*_{Val}$ and $D^*_H \equiv D^*_{CD\ or\ CDNP}$, and the green and orange dashed lines show D_H and D_G, respectively. The definitions of these symbols are shown in Eq 1. Comparing the dashed and solid orange lines, D_H and D^*_H are almost invariant to the binding because of consumption of molecular weight guest into the large molecular weight host. On the other hand, D^*_G was dramatically decreased upon the binding. When the decrease in D^*_G is defined by $\Delta D_G = D_G - D^*_G$, Figure 2-5 shows ΔD_G of βCDNP >> ΔD_G of βCD

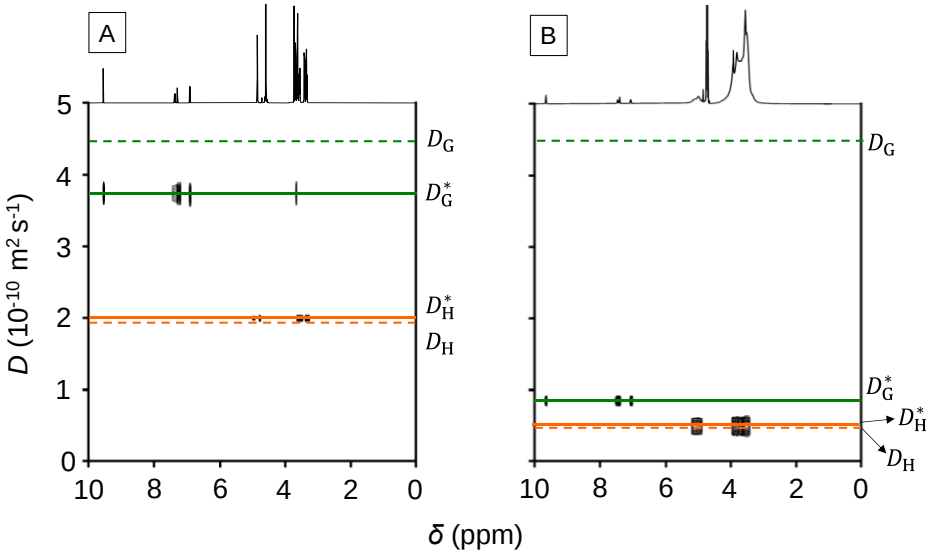

Figure 2-5. Examples of 2D DOSY comparing βCD/Val (A) and βCDNP$_{2.7}$/Val (B) systems. The horizontal axis represents chemical shifts, whereas the vertical axis diffusion coefficients; the dark spots are the resonances of the aqueous solution of the inclusion complex spread in the second dimension according to their measured diffusion coefficient.

2-3-4. Discussion

Based on the results of the Job plots in Figure 2-2, it can be concluded that vanillin is taken up by βCDNP in the same mode (i.e., 1:1 binding) as βCD. DOSY indicated the large increase in K due to the polymerization. The same increase in K was confirmed by fitting the Job plot with Eq 5. ROESY and NOESY in Figure 2-3 indicated that the vanillin molecule enters more deeply into the βCD cavity in βCDNP than in βCD, while its molecular orientation (the

phenolic end nearer to the lower rim and the aldehyde end nearer to the upper rim of βCD) may be maintained in βCDNP. In this section, we discuss how the *K* value is affected by the nature of the host molecules: differences of CD ring and ECH/CD. Based on the obtained data, we speculate on the molecular origin of the increase in *K*. Incidentally, it is well known that *K* can be expressed by the ratio of the association (k_a) and dissociation (k_d) rate constants in the 1:1 binding model:

$$K = \frac{k_a}{k_d} \tag{6}$$

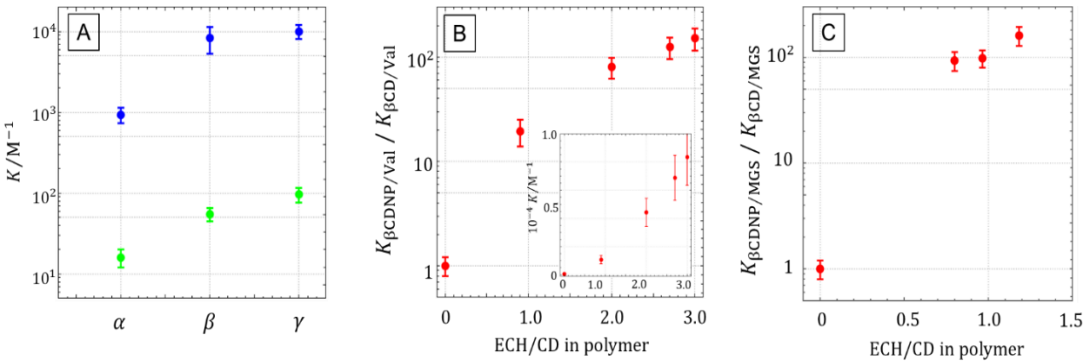

Figure 2-6. Summary of DOSY experiments. A: The binding constants are plotted for the three CDs (green) and αCDNP$_{3.2}$, βCDNP$_{3.0}$, and γCDNP$_{3.0}$ (blue). B: $K_{\beta CDNP/Val}$ values were divided by $K_{\beta CD/Val}$ and plotted against ECH weight percent in CDNPs; the inset shows the increase of $K_{\beta CDNP/Val}$. C: The same plot as in B was constructed for MGS-CDNPs using the published data[1].

Figure 2-6A compares the *K* values among three types of CDs and CDNPs. *K* of CD increased in the order of α < β < γ, namely 16, 55, and 97 M^{-1} respectively. Several works have determined the *K* value between βCD and vanillin (hereinafter denoted as $K_{\beta CD/Val}$). Ferrazza et al[73] obtained $K_{\beta CD/Val}$ = 142 ± 9 M^{-1} using DOSY in the solution similar to those in the present study. Two other groups carried out ^{1}H NMR titration, similarly to the present Job plot, to obtain $K_{\beta CD/Val}$ = 74–172 M^{-1}.[77, 84] Their values are at most three times larger than ours, but we do not know the reason for this discrepancy. On the other hand, Karathanos et al[76] obtained $K_{\beta CD/Val}$ = 5.3 M^{-1} using the solubility method, which is much smaller than our values. As shown in Figure 2-2, we obtained $K_{\beta CD/Val}$ = 95 M^{-1} using Job's plot of NMR. We suppose that the absolute value of *K* may

depend on the method and experimental conditions used. In particular, vanillin tends to aggregate even at a low concentration, which may affect the ability to determine *K* accurately. A notable feature in Figure 2-6A is the dramatic increase in *K* value due to the polymerization. The increment of *K* for $\beta CDNP_{2.7}$ (denoted by $K_{\beta CDNP2.7/Val}$) is approximately 125 times. $\alpha CDNP_{3.2}$ and $\gamma CDNP_{3.3}$ also showed large increases of around 60 and 100 times, respectively.

Figure 2-6B plots the ratio of $K_{\beta CDNP/Val}/K_{\beta CD/Val}$ against ECH/CD. It is worth noting here that *K* increases almost exponentially with the increase in ECH/CD, consistent with our previous study on the MGS/βCDNP system as shown in Figure 2-6C.[1] This means that the ECH matrix in the particles significantly contributes to the increase in *K*. However, DXNP (dextran based ECH polymer) has no ability to interact with vanillin (see the Figure S5 in the supplementary information) and βCDNP shows the same 1:1 binding mode with βCD. These two facts indicate that CD is essential in the interaction and the ECH matrix does not directly ingest the guest, but it helps increase the CD/guest interaction.

Figure 2-7 compares the *K* values of βCD, $\beta CDNP_{0.9}$, and βCDNP2.7for vanillin and its two analogs. Vanillin has an aldehyde group, while the others have a carboxyl group and VMA has an additional hydroxyl group. Therefore, the order of hydrophobicity would be as follows: vanillin > HVA > VMA. The most hydrophobic vanillin shows the largest increment of *K* due to the ECH polymerization, suggesting that the hydrophobic interaction may play an important role in the enhancement of *K*. The native CD has several hydroxyl groups on the upper rim, which may obstruct the hydrophobic guest from entering the inner cavity of CD. ^{1}H-NMR of $\beta CDNP_{0.9}$ in DMSO showed that the polymerization converted all of the hydroxyl groups to esters. Therefore, there is nothing obstructing ingestion of the hydrophobic guests for CDNPs. This factor may increase k_a in Eq 6. This may be one reason for the enhancement of *K*. CD molecules are connected by the ECH network in CDNPs. Before the guest molecules are captured by CD, they may be located at the ECH network. The polymerized ECH is hydrophobic and thus they may attractively interact with

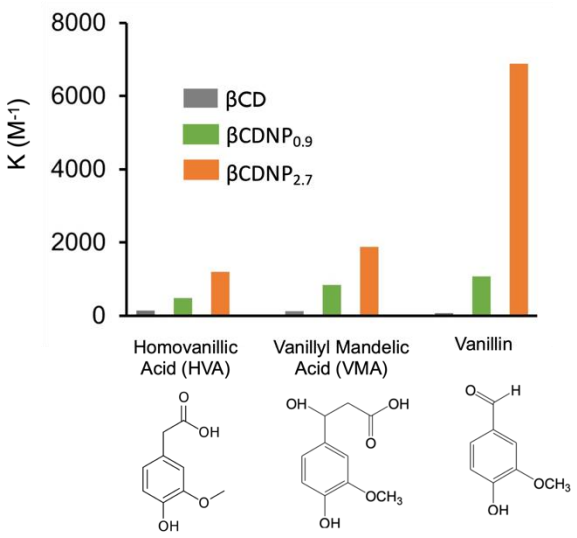

Figure 2-7. Increase of the binding constants for vanillin analogs.

the guest molecules, which increases the local concentration of the guest molecules in the vicinity of the CDs in CDNPs. Furthermore, the hydrophobic interactions of the ECH network slow down the diffusion of vanillin and make the guest readily available for interaction with the CD cavity. These factors may decrease k_d in Eq 6 and thus increase K. We did not see any direct interaction between the ECH network and vanillin. However, the large ECH/CD polymers show deviation from the 1:1 binding model and further increase in K as shown in the Appendix A (Figure A3), which suggests that the ECH network can interact with vanillin.

Before concluding, we would like to present a good example of the enhanced binding of βCDNP. Alsbaiee et al[87] reported in Nature that a polymerized CD showed dramatically increased absorption of bisphenol A (BPA), comparable to that of active carbons. This finding made a profound impact on water-purification technology and green chemistry. They used 2,3,5,6-tetrafluoroterephthalonitrile as a linker of CDs, which is not environmentally friendly because it contains fluorine and is also expensive. We recently found that our βCDNP polymers (although we used water-insoluble βCDNP, which is synthesized by the crosslinking reaction between βCD and ECH in the presence of sodium dodecyl sulfate in this case, denoted as βCDNP-SDS[88]) can exhibit comparable performance to their polymers, as shown in Figure 2-8. Interestingly,

βCDNP shows better adsorption behavior with granular activated charcoal; however, its surface area is much smaller than that of activated charcoal.

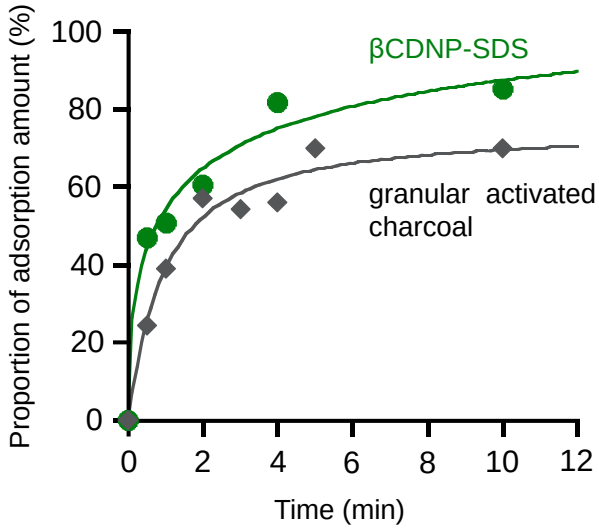

Figure 2-8. Time-dependent adsorption of aqueous bisphenol A (0.1 mM) by granular activated charcoal (Cat. No. 01084–12, supplied by Kanto Chemical Co.) and βCDNP-SDS (1 mg/ml). The BPA encapsulation experiments were performed under the following conditions: βCDNP-SDS content (or granular activated charcoal) of 18 mg and temperature of 298 K. The Brunauer-Emmett-Teller (BET) surface areas of the granular activated charcoal and βCDNP-SDS are 1400 and 0.2 $m^2 g^{-1}$, respectively.

2-3-5. Conclusion

Several water-soluble CDNPs were produced by cross linking reactions between CDs molecules and different amounts of ECH in aqueous solutions. Detailed structural characterization and investigation of the binding constants of the CDNPs for vanillin and its analogs in aqueous solutions were performed. Our NMR findings clearly indicate that vanillin is more efficiently complexed with CDNPs than native CDs, with stronger binding affinity. This demonstrates that these water-soluble cyclodextrin polymers have great potential for various food, environmental, and pharmaceutical applications. In addition, DOSY NMR is useful as an alternative tool for the initial assessment of the enhanced binding constant of CD-based materials.

Chapter 3. Molecular mechanism of the interaction between β-cyclodextrin-based nanoparticles (βCDNPs) and paroxetine hydrochloride

3-1. Introduction

Nanoparticles have emerged as one of the promising drug delivery systems to increase the bioavailability of the hydrophobic small molecules with biological activity: enhancing their biocompatibility with the hydrophilic cellular atmosphere of the body, thus reducing toxicity and increasing therapeutic efficacy.[89] Among them, cyclodextrin-based nanoparticles (CDNPs) have shown great potential as versatile carriers for drug delivery systems. Cyclodextrins (CDs) are shaped like a cone with a hydrophilic exterior and a hydrophobic interior. The hydrophobic interior can form host-guest complexes with a wide variety of hydrophobic drugs. This complexation may be particularly useful for increasing the solubility and stability of hydrophobic drugs (Figure 2- 1A). There are three main types of cyclodextrins: α-, β-, and γ- CDs, which are composed of 6, 7, and 8 glucose units, respectively. Each type has different dimensions of the inner cavity that determines the molecules they can enclose and the binding affinity. For intravenous administration, cyclodextrins have been used in several approved drugs.[90,91] However, it is well known that high doses of CDs can lead to nephrotoxicity in animals. [92] This is particularly true for β-cyclodextrin (βCD). It is considered that βCD forms a complex with cholesterol after extracting the cholesterol present in the cell membrane, and toxicity arises due to the aggregation of that complex.[93] CDNPs seem not to have such a toxicity because of increased solubility with water. Nanoparticles including CDNPs can accumulate in tumor tissues due to the EPR effect,[94] a unique phenomenon observed dependently on the size of nanoparticles. This can be advantageous for cancer drug delivery. Furthermore, improved drug loading and controlled release are expected for CDNPs. These are main reasons that CDNPs are studied as DDS.

In our previous studies, we cross-linked CDs using epichlorohydrin (ECH) at a dilute condition to prepare the CDNPs that can be easily dispersed in water

without formation of large aggregates. The particle size of our CDNPs was controlled less than 20 nm. The CD weight percent in CDNPs were well controlled by changing the epichlorohydrin, ranging from 50 to 90 %. We found that α-Mangostin (MGS), a xanthone derivative known for its anti-cancer efficacy and extracted from the pericarps of mangosteen, can be incorporated into CDNPs at a much higher loading ratio than with CDs alone.[95,96] Later, we confirmed the enhanced binding of CDNPs with diffusion-ordered spectroscopy nuclear magnetic resonance (DOSY-NMR). The optimization of drug

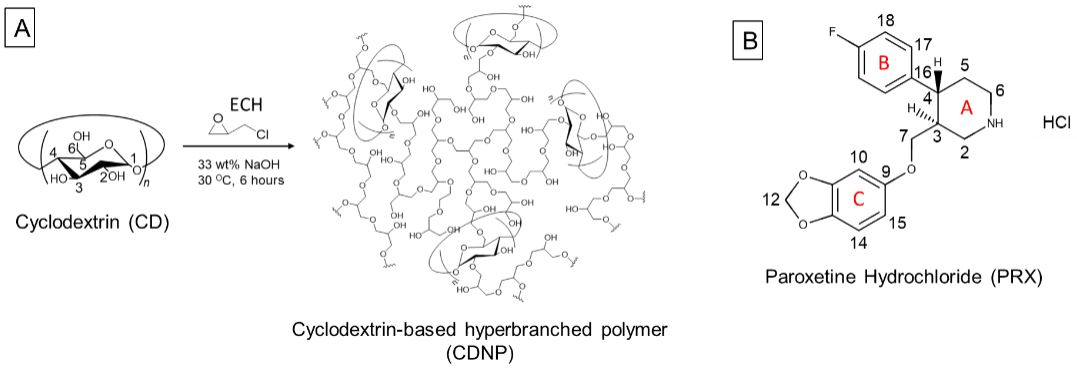

Figure 3-1. Chemical structures and proton numbers of PRX and cyclodextrin (CDs). A: Synthesis scheme of cyclodextrin-based hyperbranched polymers (CDNPs) through polyaddition reactions with ECH. B: The chemical structure of PRX.

encapsulation by CDNPs requires a detailed understanding of the binding interactions between the guest drug and the nanoparticle. Therefore, finding a reliable method to accurately determine host-guest interaction constants (*K*) is essential. Several methods are currently used for the measurement of binding constants, such as isothermal titration calorimetry (ITC), optical spectroscopy, and nuclear magnetic resonance spectroscopy (NMR).[97] However, the selection of an appropriate method depends on several parameters such as the solubility, size, and properties of the guest molecule and the host molecules.

DOSY-NMR is a powerful technique used to investigate molecular interactions in a complex mixture. This technique allows the separation of signals of different species based on their diffusion coefficient, and therefore, it is capable of providing information about the binding constants.[98, 79] DOSY-NMR offers several advantages, including non-destructive and real-time measurements.

These characteristics make it a valuable tool for studying molecular interactions and diffusion processes. By employing DOSY-NMR, we can investigate the impact of various factors, such as temperature, pH, and nanoparticle formulation, on the binding constant between CDNPs and drugs. Several studies have demonstrated the usefulness of DOSY-NMR for the investigation of host-guest interactions in various systems, including CDs and encapsulated drugs.[39,40,99,100] However, it is not without its drawbacks.[101,102] One major drawback is the experimental complexity associated with DOSY-NMR. Setting up and executing the experiments can be technically challenging, requiring specialized pulse sequences and gradient setups that may not be available in common NMR spectrometers. Additionally, DOSY-NMR experiments typically suffer from reduced sensitivity compared to traditional NMR experiments, leading to lower signal-to-noise ratios and higher detection limits for low-concentration compounds, necessitating larger sample volumes and sufficient compound solubility. Besides, the sample must be stable during the long acquisition times needed for diffusion encoding, which can be problematic for unstable or reactive compounds. Analyzing DOSY-NMR data can also be complex and time-consuming, requiring sophisticated data processing methods and specialized software tools. In addition, the presence of convection in DOSY-NMR experiments can introduce additional motion and distort diffusion measurements leading to inaccurate estimation of diffusion coefficients. Moreover, DOSY-NMR is generally more applicable to molecules within a specific size range and may encounter challenges when dealing with large or small molecules. NMR diffusion measurements provide a versatile and powerful means of quantifying diffusion coefficients across an impressive range of over ten orders of magnitude, stretching from 10^{-5} to 10^{-15} m^2s^{-1}.[103] This remarkable capability enables the investigation of diffusion processes ranging from gases to substantial polymeric structures. For large molecules like macromolecules, polymers, or aggregates, their diffusion coefficients can be relatively low due to their size and complex structure, resulting in broader and less resolved peaks in the DOSY spectrum. The overlap of signals from different components further complicates the

accurate determination of individual diffusion coefficients and quantitative analysis. Despite these drawbacks, with careful experimental design and advanced data analysis techniques, DOSY-NMR remains a valuable tool for studying mixtures and molecular diffusion.

In this study, we aimed to determine the binding constant of paroxetine hydrochloride hemihydrate (PRX, Figure 2-1B), an antidepressant drug, with native cyclodextrin and our CDNPs made from β-CD and ECH, using ITC and DOSY-NMR, respectively. PRX is a family member of selective serotonin reuptake inhibitors that can be used to treat depression. As shown in Figure 1B, PRX comprises the piperidine A-ring, the 1,3-benzodioxole moiety C ring, and the 4-fluorophenyl B-ring. The ether linkage between the A and C rings provide almost free rotation of the C ring, while the A and B rings are almost perpendicularly aligned due to the steric hindrance. Being obvious from the PRX structure, PRX is very hydrophobic, and to improve the drug bioavailability, cyclodextrin encapsulation has been studied by many groups.[104,105,106] As far as we know, there has been no work to study the inclusion of phenomena between PRX and CDNPs. As mentioned above, we have a series of CDNPs that can increase the bioavailability of hydrophobic drugs. Our main aim of this study is to examine the binding phenomena between our CDNPs and PRX.

3-2. Experimental

3-2-1. Materials

Paroxetine hydrochloride hemihydrate (PRX) (purity > 98%) was supplied by Tokyo Chemical Industry Co. (Tokyo, Japan), and used without further purification. β-cyclodextrins (βCD) and epichlorohydrin (ECH) (purity > 99%) were purchased from Tokyo Chemical Industry Co. (Tokyo, Japan), and used without further purification. Deuterium oxide (99.8%) was obtained from Fujifilm Wako Pure Chemical Co. (Osaka, Japan). All other chemicals and solvents used were commercially available and used as received. The CDNPs utilized in this study was synthesized via a condensation reaction between βCD and ECH under an alkaline condition, following the same method as described in the previous work.[40]

3-2-2. NMR measurements

All NMR experiments were performed on a JEOL JNM-ECZ500R spectrometer operating at 500 MHz with a stationary magnetic field of strength 11.74 T at the analytical center of the University of Kitakyushu. All tested solutions were prepared 1 day before the measurements to ensure complete solubilization. For the ^{1}H NMR experiment, the concentrations of PRX and βCD were both set to 10 mM. Two-dimensional nuclear rotating frame overhauser effect spectroscopy (ROESY) experiments was performed to characterize the structure of βCD complexes formed with PRX. ROESY NMR spectra was acquired using a standard pulse sequence from the JEOL library at 298 K. The relaxation delay between successive pulse cycles and mixing time were 3.3 s and 0.3s, respectively.

Diffusion coefficients were obtained through DOSY experiments using a bipolar pulse paired longitudinal eddy current delay (BPP-LED) sequence at 293 ± 0.5 K in 5 mm tubes. In the DOSY experiments, the concentrations of PRX, βCD were all set to 10 mM. The duration of the magnetic field pulse gradients δ was 3 to 3.4 ms, depending on the specific sample. The pulse gradient strength was increased from 30 to 300 T/m. The diffusion times were optimized between 0.1

s for PRX and 0.15 s to 0.3 s depending on the sample to completely decrease the signals by a factor of 10–20 and better analyze the exponential signal decay. Following the measurements, the DOSY experimental data were processed using Delta 5.3 software (JEOL Ltd., Tokyo, Japan). Baseline correction, phase correction, and Fourier transformation were performed, and the diffusion coefficients were obtained by fitting the peak intensity $I(G_z)$ to the exponential decay curve, in accordance with the Stejskal-Tanner equation. [79]

The diffusion coefficient (D) for the solution was determined by calculating the average of the diffusion coefficients of multiple proton species. To visualize the data in a two-dimensional format, an inverse Laplace transformation was applied to the Y-axis for each data point, after Fourier transformation along the X-axis.

3-2-3. Estimating the binding constant from DOSY experiment

Same as described in Chapter 1, Section 1-3-5.

3-2-4. Job plot to determine the stoichiometry and binding constant

We used the continuous variation method (Job plot) with NMR to determine the stoichiometry of the complexation between βCD, $\beta CDNP_{2.7}$, and PRX. A set of PRX-βCD and PRX-$\beta CDNP_{2.7}$ solutions was prepared by varying the molar fraction of PRX from 0 to 1, while maintaining a total concentration of 4.9 mM of PRX-βCD and PRX-$\beta CDNP_{2.7}$. The stock concentrations of PRX, βCD and $\beta CDNP_{2.7}$ were all 4.9 mM. Here, the concentration of $\beta CDNP_{2.7}$ is calculated based on the βCD units in $\beta CDNP_{2.7}$. All of the ^{1}H-NMR measurements were conducted at a temperature of 298 K. The obtained data points were fitted using the equation for a 1:1 binding mode:[107]

3-2-5. ITC experiment

The thermodynamics of the binding interaction between βCD, CDNPs, and PRX were investigated using isothermal titration calorimetry (ITC). This measurement provided insight into the various molecular forces that affect the formation of the inclusion complex between the host and guest molecules. ITC has gained significant attention for studying molecular interactions as it offers

direct access to the measurements of Gibbs free energy (ΔG), enthalpy (ΔH), entropy (ΔS), and equilibrium binding constant (*K*) from a single experiment. The binding enthalpogram of the PRX-βCD and PRX-βCDNPs systems were analyzed and various thermodynamic parameters, such as ΔG, ΔS, ΔH, and binding constant value were obtained after necessary corrections.

ITC measurements were conducted at 298 K on a VP-ITC MicroCalorimeter ultrasensitive titration calorimeter manufactured by MicroCal, LLC. Calorimetric titration experiments were carried out at constant temperature by injecting 9.5 mM PRX solution into the sample cell containing 1 mM βCD or CDNPs, while maintaining a fixed stirring speed of 250 rpm. The titration parameters, including the number of injections (34), volume of each injection (8 μL), and injection duration (20s), were input into the data control software. The aqueous solutions in the cell were stirred by the syringe at a speed of 307 rpm. The titrant volume was injected in controlled pulses with a 300 s interval between injections from a 250 μL injection syringe into the sample cells. The sample cell volume was 1.3611 mL. To correct the integrated heat effects of each injection, the corresponding integrated heat effects of dilution of the drug and cyclodextrin were subtracted. This involved subtracting the heat effect of injecting the drug solution into water and the heat effect of injecting water into the cyclodextrin solution, respectively.

The experimental data obtained from the calorimetric titration were analyzed using Origin software, based on a model of a single set of identical binding sites. In this model, it is assumed that the ligand and receptor interact through a single type of binding site, and all binding sites have the same affinity for the ligand. The binding constant *K* is described by:

$$K = \frac{\Theta}{(1-\Theta)[X]} \tag{7}$$

$$X_t = [X] + n\Theta M_t \tag{8}$$

where Θ is fraction of sites occupied by ligand X, X_t and $[X]$ are bulk and free concentration of ligand, M_t and $[M]$ are bulk and free concentration of macromolecule in active cell volume V_o and n is number of sites.

Combining Eq. 7 and Eq. 8 above gives:

$$\Theta^2 - \Theta\left[1 + \frac{X_t}{nM_t} + \frac{1}{nKM_t}\right] + \frac{X_t}{nM_t} = 0 \qquad (9)$$

The total heat content Q of the solution contained in V_o (determined relative to zero for the unliganded species) at fractional saturation Θ is:

$$Q = n\Theta M_t \Delta H V_o \qquad (10)$$

where ΔH is the molar heat of ligand binding. Solving the quadratic Eq. 9 for Θ and then substituting this into Eq. 10 gives:

$$Q = \frac{nM_t\Delta HV_o}{2}\left[1 + \frac{X_t}{nM_t} + \frac{1}{nKM_t} - \sqrt{\left(1 + \frac{X_t}{nM_t} + \frac{1}{nKM_t}\right)^2 - \frac{4X_t}{nM_t}}\right] \qquad (11)$$

The calculated value of Q, denoted as Q(i), can be determined at the end of the ith injection for any designated values of n, K, and ΔH. However, when comparing with experimental data, the parameter of interest is the change in heat content from the completion of the i-1 injection to the completion of the ith injection. The expression for Q in Eq. 11 only applies to the liquid contained in volume V_o. Hence, after completing an injection, a correction must be applied for the displaced volume (i.e., ΔV_i = injection volume) since some of the liquid in V_o after the i-1 injection will no longer be in V_o after the ith injection, even though it will contribute to the heat effect (assuming the kinetics of reaction and mixing are fast) before it passes out of the working volume V_o. The liquid in the displaced volume contributes about 50% as much heat effect as an equivalent volume remaining in V_o. Therefore, the correct expression for the heat released, $\Delta Q(i)$, from the ith injection is as follows:

$$\Delta Q(i) = Q(i) + \frac{dV_i}{V_o}\left[\frac{Q(i) + Q(i-1}{2}\right] - Q(i-1) \qquad (12)$$

The fitting of experimental data involves several steps. Firstly, initial estimates for the values of n, K, and ΔH are made, which can often be obtained accurately using software like Origin. Secondly, $\Delta\, Q(i)$is calculated for each injection and compared with the measured heat for that specific injection in the experiment. Thirdly, the initial values of n, K, and ΔH are refined using standard Marquardt methods. Lastly, the procedure is iterated until no significant improvement in the fit is achieved with further interactions.

3-3. Results and discussion

3-3-1. Polymer characterization

The average molecular weight (M_w) was determined to be 7.29×10^4 g/mol using size exclusion chromatography coupled with multiangle light scattering (SEC-MALS). The hydrodynamic radius (R_h) was measured as 3.5 nm using dynamic light scattering, and 3.9 ± 0.2 nm using DOSY. The weight percentage of CD was determined using the phenol sulfuric acid method and, when combined with M_w, was converted into the number of CDs per CDNP particle (N_{CD}), resulting in a value of 17. We have verified that the phenol sulfuric acid technique can accurately estimate the weight percentage of CD with a margin of error of around 5%. Additionally, when applying this method, we found that the ECH polymer without CD exhibited no detectable carbohydrates, indicating a 0% carbohydrate content. The results are summarized in Table I and this CDNP was denoted $\beta CDNP_{2.7}$.

Table 3-1. Sample list used in this work, including the molecular characteristics determined by GPC-MALS and the phenol sulfuric acid method.

Sample code	Feeding weight ratio[a]	M_w (g/mol)[b]	R_h (nm)[c]	N_{CD}[d]	*wt%* CD (%)	ECH/CD in polymer (w/w)
$\beta CDNP_{2.7}$	4.25	7.29×10^4	3.5	17	26.7	2.7
$\beta CDNP_{0.9}$	2.84	9.37×10^4	4.0	44	53.0	0.9
$\beta CDNP_{0.7}$	4.25	1.98×10^4	1.9	10	57.1	0.7
$\beta CDNP_{0.4}$	1.42	2.28×10^4	2.3	14	70.4	0.4

a) The feeding weight ratio is the weight ratio between ECH and CD in the synthesis reaction. ECH/CD in the polymer is the weight ratio between ECH and CD in the polymer

b) Determined by GPC coupled with SLS, the estimated error range is about ±3 –±5%

c) Determined with DLS

d) From the phenol sulfuric acid method, the estimated error range is about ±5%

Table 3-1, show the molecular characteristics of $\beta CDNP_{2.7}$. The particle size and surface properties are the most important parameters for blood-injectable drugs.[108] There are intensive studies by McNeil et al. [109] According to their findings, particles larger than approximately 200 nm in diameter are rapidly cleared from the bloodstream by the liver and spleen, while particles under 10 nm are quickly eliminated by the kidneys. Therefore, the particle sizes are

designed to be within the range of about 10-100 nm in diameter to avoid rapid clearance. Furthermore, the surface properties play an important role in stabilizing the particle in blood. Hydrophobic and positively charged surfaces tend to attract more proteins, a phenomenon known as "opsonization", compared to neutral hydrophilic surfaces. This can lead to rapid recognition and clearance of the nanoparticles by the immune system, reducing their circulation time. Although the size of βCDNP2.7is close to the lower limit, our previous paper demonstrated that βCDNPs have a longer blood circulation time.[110] This is presumably attributed to their almost neutral charge and sugar-coated surface. We also demonstrated that the binding constant between βCDNP and the host is determined by the ECH/CD ratio in the polymer (which is the weight ratio of ECH to CD determined by the CD weight percent), and a ratio of ECH/CD = 3.0 yields the largest binding constant. It is important to note that reaction conditions with ECH/CD > 3.0 did not yield molecularly dispersed particles.[95] Therefore, we can expect that βCDNP2.7shows the highest level of the binding.

3-3-2. 2D ROESY spectra of the complex

Figure 3-2A displays the 1H-NMR spectra of PRX, βCD, $βCDNP_{2.7}$, a mixture of PRX and βCD, and a mixture of PRX and $βCDNP_{2.7}$(both samples having a βCD/PRX molar ratio of 1:1) in D_2O. The area enclosed by a square in A where the many PRX protons have peaks are magnified in Figure 3-2B and 2C. It is evident that complexation with βCD and $βCDNP_{2.7}$ caused changing chemical shift in the proton peaks. The chemical shifts of protons and their differences between the free and complex forms are presented in Table 2, using the numbering scheme illustrated in Figure 3-1. The proton peaks of PRX observed in our study were in agreement with the data previously reported in the literature.[105] Bernine et al carried out ^{1}H and ^{13}C NMR on the complex of PRX and βCD in order to define the stoichiometry and their binding constant.[105] They conclude that the C-ring of PRX is deeply inserted in the CD cavity, while the B ring lays above the wider rim and the confirm the 1:1 binding (form I as shown in Figure 3-2D). More recently, Aree reported X-ray crystallography combined

with the density functional theory (DFT) calculation for the βCD-PRX complex.[104] According to the results, βCD and PRX can take a new form called form II (as shown in Figure 3-2D) in which the B-ring is inserted into the CD cavity and the stoichiometry is [βCD]:[PRX]=2:1. Figure 3-2C shows that the PRX peak of proton H12 becomes doublet after the complexation with both βCD and $\beta CDNP_{2.7}$. However, the direction of the chemical shifts due to the complexation is quite different; for example, as shown in Figure 3-2C, the PRX peak of proton H12 were spitted after complexation with βCD and both peaks showed down-field shift, while the same protons were spitted, but a high-field shift was observed for the $\beta CDNP_{2.7}$ complexation. The chemical shifts for the PRX proton peaks H14 and H17 also exhibited the same trend: an upfield shift in the βCD-PRX complex and a downfield shift in the $\beta CDNP_{2.7}$-PRX complex. This suggests distinct molecular interactions between βCD-PRX and $\beta CDNP_{2.7}$-PRX. There is a possibility that within CDNP, two CDs form a complex with a single PRX molecule, with one CD capturing the B-ring and the other CD capturing the C-ring.

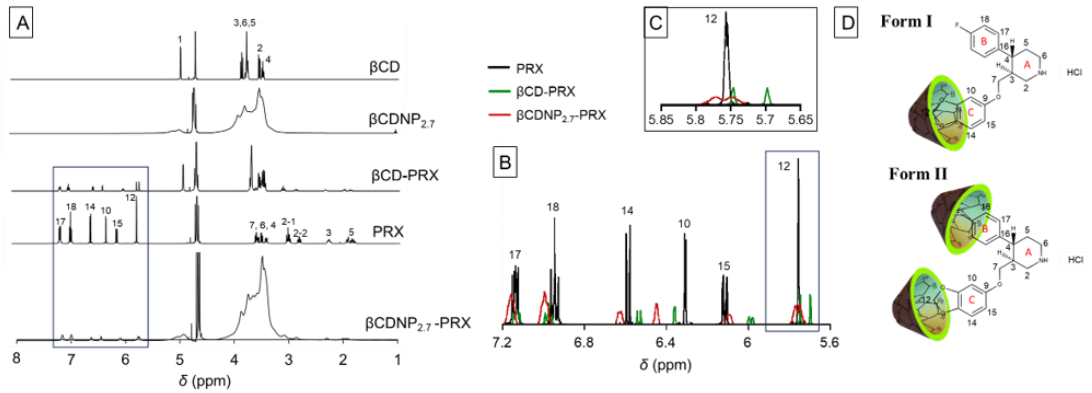

Figure 3-2. ^{1}H-NMR spectra of PRX, βCD, $\beta CDNP_{2.7}$, and βCD-PRX and $\beta CDNP_{2.7}$-PRX mixtures. The intermediate δ regions of the spectra are enlarged in part B. A: ^{1}H NMR spectra of PRX, βCD, $\beta CDNP_{2.7}$, βCD-PRX and $\beta CDNP_{2.7}$-PRX mixtures. B, C: The intermediate δ regions from 5.6 to 7.2 ppm (B) and 5.65 to 5.85 ppm (C) of the ^{1}H-NMR spectra of PRX, and βCD-PRX and $\beta CDNP_{2.7}$-PRX mixtures. D: Three-dimensional structure of CD-PRX complex (Form I: CD/PRX formation; Form II: CD_2/PRX formation)

Figure 3-3 displays the ROESY spectra of βCD-PRX and $\beta CDNP_{2.7}$-PRX. In the βCD-PRX spectrum, distinct intermolecular dipolar interactions are evident between the protons of the B and C rings (H12, H15, H10, H14, H17, H18) of PRX and the protons within the βCD cavity. Notably, the interaction involving

proton H12 of PRX and the CD cavity is exclusively observed in the βCD-PRX complex. This observation suggests a profound insertion of the C-ring of PRX into the CD cavity within the βCD-PRX complex. In the case of $\beta CDNP_{2.7}$-PRX, the interactions between the proton H17 of PRX and the protons of the A ring (H2, H3, H5) of PRX are observed. This observation suggests that when PRX forms a complex with CDNP, the molecule undergoes deformation, potentially bringing proton H17 closer to the A ring.

Table 3-2. Proton chemical shift data (ppm) of PRX, βCD, $\beta CDNP_{2.7}$ in the free state and in the complex (d: doublet, t: triplet, q: quadruplet, m: multiplet)

	δ Free	δ Complex βCD	δ complex $\beta CDNP_{2.7}$	$\Delta\delta_{CD/PRX}$	$\Delta\delta_{CDNP/PRX}$
PRX					
H17 (2H,t)	7.137	7.129	7.161	-0.008	0.024
H18 (2H,t)	6.947	6.976	6.995	0.029	0.048
H14 (1H,d)	6.579	6.525	6.627	-0.054	0.048
H10 (1H,d)	6.307	6.358	6.449	0.051	0.142
H15 (1H,dd)	6.109	5.981	6.093	-0.128	-0.016
H12 (2H)	5.755	5.697	5.771	-0.058	0.016
	5.757	5.746	5.748	-0.011	-0.009
H7 (2H,qd)	3.578	3.499	overlapped	-0.079	-
H6 (2H,q)	3.491	overlapped	overlapped	-	-
H4 (1H,dt)	3.402	overlapped	overlapped	-	-
H2-1 (1H,m)	3.004	3.097	3.08	0.093	0.076
H2-2 (1H,td)	2.815	2.862	2.857	0.047	0.042
H3 (1H,m)	2.281	2.325	2.298	0.044	0.017
H5-1 (1H,dq)	1.934	1.985	1.995	0.051	0.061
H5-2 (1H,qd)	1.838	1.866	1.913	0.028	0.075
β-CD					
H1 (1H,d)	4.929	4.900		-0.029	
H3 (1H,t)	3.828	3.697		-0.131	
H6 (1H)	3.740	3.667		-0.073	
H5 (1H)	3.720	3.661		-0.059	
H2 (1H, dd)	3.504	3.525		0.021	
H4 (1H, t)	3.447	3.453		0.006	

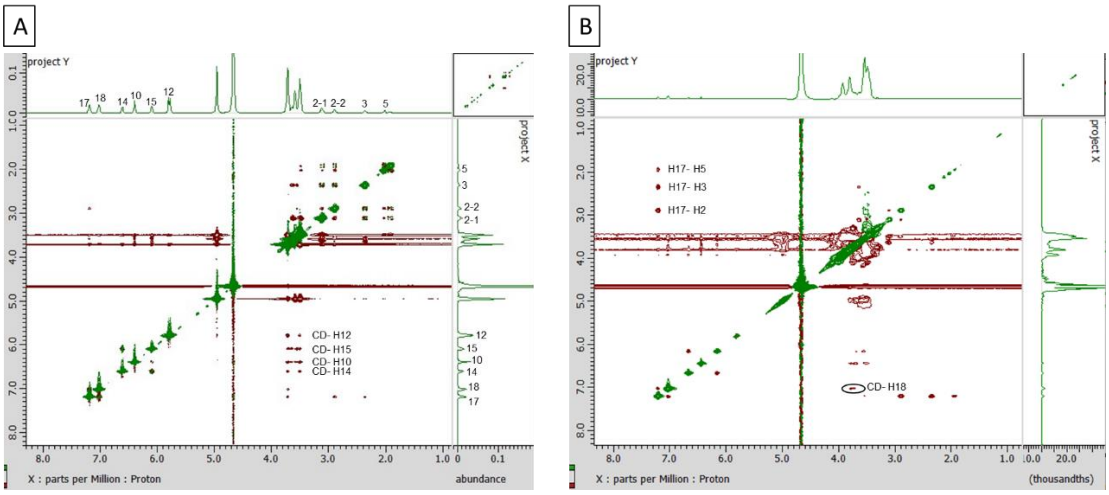

Figure 3-3. The 2D ROESY spectra of βCD-PRX (A) and βCDNP$_{2.7}$-PRX (B) solutions at 298K: the molar ratio of PRX:βCD was 1:1 and the concentrations of all of PRX, βCD, and βCD in βCDNP$_{2.7}$ were 10 mM.

3-3-3. Job plots to determine the binding constant of the complex

In solution, the stability of the 1:1 βCD and PRX inclusion complex has been suggested by combining NMR and molecular dynamics (MD) simulation. Bernini et al. (2004) reported a binding constant of approximately 2000 M^{-1} for this complex.[105] To further validate the results, a Job plot was constructed for βCD and βCDNP$_{2.7}$ with PRX using the chemical shift of the H14 proton as shown in Figure 3-4A and 4B. The difference in chemical shifts of the complex and guest molecules in the absence of the host was denoted as $\Delta\delta_{HG} = \delta_{HG} - \delta_G$. The plot depicted $[G]_i\Delta\delta_G$ against r, where $[G]_i$ represents the total concentration of the guest molecule (PRX) in the presence of both free and complexed forms, and $\Delta\delta_G$ represents the difference in chemical shifts of the guest molecule with and without the host at a given composition ratio r. The composition ratio r was defined as $r = [G]_i/([G]_i + [H]_i)$, with $[H]_i$ representing the concentration of CD in the solution. The total concentration of $[G]_i + [H]_i$ was maintained at a constant value of 4.9 mM.

The analysis revealed that the $[G]_i\Delta\delta_G$ value reached its peak at r = 0.5, indicating a 1:1 binding ratio for βCD and PRX. Thus, the data points were fitted using Eq 5 that corresponds to this particular binding mode. The analysis confirmed a 1:1

binding ratio and a binding constant of approximately 2000 M^{-1} between βCD and PRX. The obtained value aligns with the binding constant reported by Bernini et al. (2004).[105]

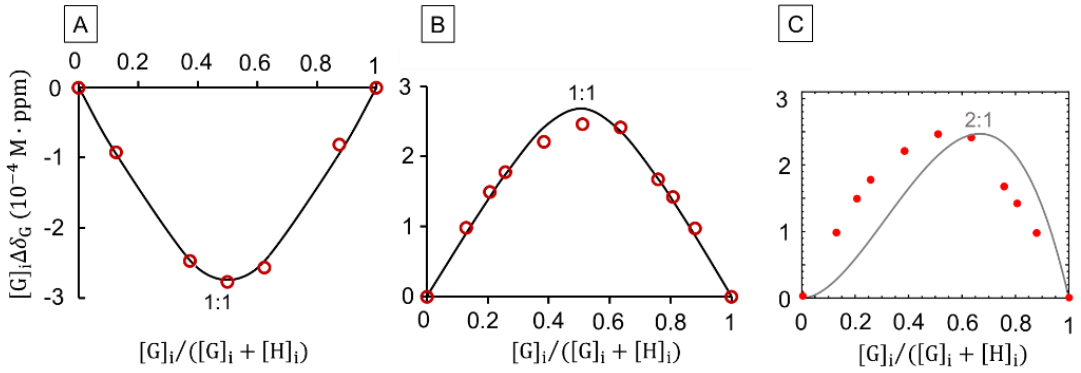

Figure 3-4. Job plot for βCD-PRX (A) in D_2O with fitting parameters K = 2000 M^{-1}, δ_{HG} = 6.52 ppm, comparing with βCDNP$_{2.7}$-PRX (B) with fitting parameters K = 3000 M^{-1}, δ_{HG} = 6.48 ppm. The total concentration $[G]_i + [H]_i$ was fixed at 4.9 mM. C: Job plot for model CD:PRX = 2:1 with fitting parameters K = 8000 M^{-1}, δ_{HG} = 8.41 ppm. Red dots are experimental data, black lines are fitting curve for 1:1 model. Gray line is fitting curve for 2:1 model.

In the case of βCDNP$_{2.7}$ and PRX, a slight deviation in the peak suggests that there may not be only a 1:1 complex in the solution. As shown in Figure 3-4C, the fitting curve for the model with a CD:PRX ratio of 2:1, with fitting parameters K = 8000 M^{-1}, δ_{HG} = 8.4 ppm, is illustrated as a gray line. The 1:1 fitting curve evidently provides a better fit to the data compared to the 2:1 fitting curve. Based on the data in Figures 4B and 4C, it indicates that the primary binding mode between βCDNP$_{2.7}$ and PRX is 1:1 complexation, but there is evidence of the presence of a 2CD:1PRX complex. Since the analysis of mixture systems can be complex, the obtained data points were fitted to a curve based on a 1:1 binding ratio (Figure 3-4B), resulting in a binding constant value of K = 3000 M^{-1}. This suggests a stronger and more favorable interaction between βCDNP$_{2.7}$ and PRX, highlighting the enhanced binding capabilities of the polymerized cyclodextrin in comparison to the individual βCD molecule.

3-3-4. Determining the binding constant of the complex with DOSY-NMR

Using the D values obtained for each peak, we generated a 2D DOSY plot in Figure 3-5 to represent the βCD-PRX (A) and βCDNP$_{2.7}$-PRX (B) sample. The peak width in the plot was determined based on the estimated error of the diffusion coefficient derived from the fitting process. In this plot, the horizontal axis represents the chemical shift of ^{1}H NMR of the mixtures, while the vertical axis represents the obtained D value. The solid green and red lines correspond to $D_G^* \equiv D_{PRX}^*$ and $D_H^* \equiv D_{CD\ or\ CDNP}^*$, respectively. Additionally, the dashed green and red lines represent D_H and D_G, respectively, as defined in Eq 1.

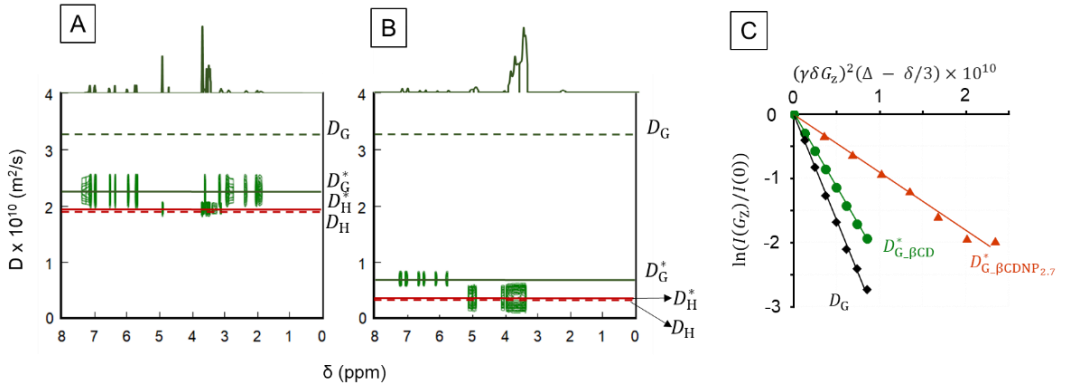

Figure 3-5. 2D DOSY-NMR comparing βCD-PRX (A) and βCDNP$_{2.7}$-PRX (B). The signal intensity ratio ln $I(0)/I(G_z)$ plotted against the exponential term in Eq 1, where $I(G_z)$ is the signal intensity at the end of the spin-echo after applying the gradient intensity of G_z and $I(0)$ is the signal intensity at the end of the spin-echo in the absence of the gradient pulse. Here, the intensity of the H17 proton of PRX is plotted.

Figure 3-5C plots ln $I(0)/I(G_z)$ against $(\gamma\delta G_z)^2$ for the H-17 proton of PRX of free PRX, PRX in βCD solution, PRX in βCDNP2.7solution. The diffusion coefficients (D) were determined from the slope and the binding constant (K) was determined using Eq 3. Table 3 presents the diffusion coefficient values of D_H, D_H^*, D_G and D_G^* in Eq 1, along with the corresponding binding constants (K values) for βCD-PRX and βCDNP$_{2.7}$-PRX. D_H and D_H^* remain almost constant, indicating that the binding of PRX to the cyclodextrin molecules has minimal influence on these diffusion coefficient values. This can be attributed to the fact that the guest molecule (PRX) is being incorporated into the larger host molecule (CD, CDNP), resulting in negligible changes in D_H and D_H^*. Based on the 1:1

model, the binding constant for βCD-PRX is determined to be 1800 M^{-1}, whereas the binding constant for βCDNP$_{2.7}$-PRX is significantly higher at 9200 M^{-1}. This highlights the notable enhancement in binding strength achieved by polymerized cyclodextrin, resulting in a remarkable 5-fold increase in the binding constant compared to non-polymerized cyclodextrin. By strengthening the interaction between the drug and its carrier, this approach fosters increased drug stability. Moreover, it significantly augments the solubility of poorly water-soluble drugs, rendering them more bioavailable and easily administered. This enhancement facilitates controlled drug release, valuable for sustaining or regulating therapeutic effects. Furthermore, stronger binding allows for the utilization of lower effective drug doses, thus mitigating potential side effects and enhancing safety.

Table 3-3. Obtained diffusion coefficient values of D_H, D_H^*, D_G and D_G^* in Eq 1 and determined K values for βCD-PRX and βCDNP$_{2.7}$-PRX.

	Diffusion coefficient (10^{-10} m^2/s)				K (M^{-1})
	D_H	D_H^*	D_G	D_G^*	
βCD-PRX	1.93	1.95	3.32	2.24	1800
βCDNP$_{2.7}$-PRX	4.4	4.31	3.32	7.16	9010

3-3-5. Thermodynamic binding of the drug with cyclodextrin

Figure 3-6 illustrates the ITC isotherms obtained at 298 K, demonstrating the interaction between PRX and βCD and $\beta CDNP_{2.7}$.

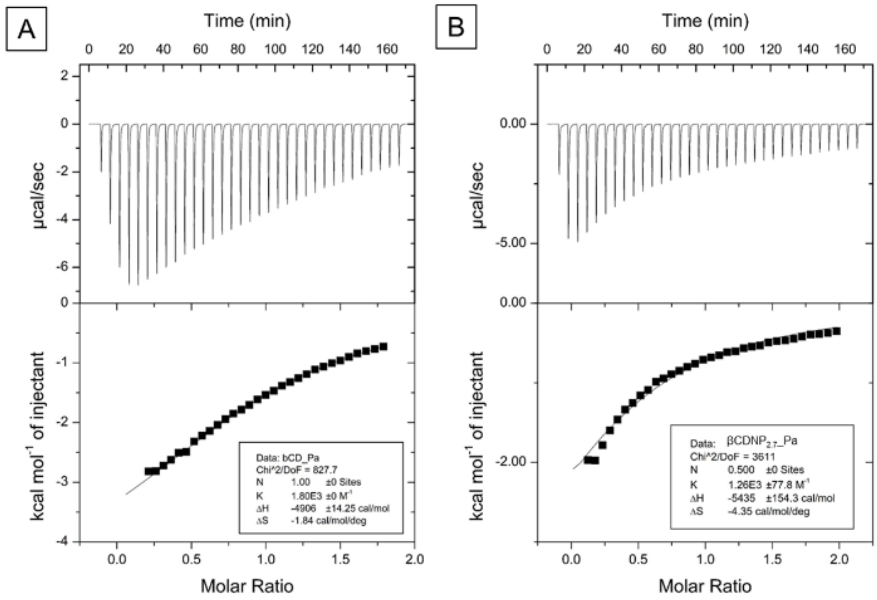

Figure 3-6. ITC isotherms for the interaction of PRX with βCD (A) and βCDNP2.7(B) at 298 K. For each titration, βCD concentration in sample cell was set at 1 mM and PRX concentration in syringe was 9.5 mM. The top panel shows the raw heats of binding generated from the mixing of PRX and βCD. The lower panel displays the binding isotherm fitted to the raw data using one site model.

The obtained thermodynamic parameters indicate an exothermic binding process, as evidenced by the negative Δ*H* value of -4906 cal/mol. The negative Δ*H* value were also observed in other studies.[111, 112, 113, 114] In aqueous solutions, negative Δ*H* values often indicate the disruption of organized water molecules within CD cavities. In aqueous solutions, the ΔH values can be associated with the disruption of organized water molecules within the cavity of CD. The observed negative ΔH value in the investigated system indicates the relocation of drug molecules within the CDs, leading to the release of structured water molecules from the CD's cavity into the surrounding bulk solution. This movement of drug molecules inside the CDs contributes favorably to the enthalpic component of the binding process. Additionally, the entropy change (ΔS) is negative with a value of -1.84 cal/mol/deg for βCD and -4.35 cal/mol/deg for $\beta CDNP_{2.7}$. The determined binding constant between βCD and PRX from the ITC measurements is 1800 M^{-1}, consistent with the binding constant determined using DOSY-NMR.

However, when attempting ITC experiment with CDNP, the best fitting curve was obtained at N = 0.5. The same results were obtained for other CDNPs as shown in Figure 3-7. The N-value indeed equals stoichiometry if the concentrations used for the fitting are correct and 100% active. However, it can also be expressed as follows:

$$N = St \times \frac{AFcell}{AFsyr} \tag{13}$$

where St is stochiometric, $AFcell$ is the active fraction in the cell, $AFsyr$ is the active fraction in the syringe. It's important to note that any of the three values in this equation can influence the N-value. This suggests potential binding ratios of 1:1 (N=1) and 1:2 (N=0.5, indicating 2 CDs to 1 PRX), or it may reflect a binding ratio of 1:2. The Job plot results indicate the likelihood of a mixture involving two complexes. This suggests that CD, after polymerization, may not exhibit 100% activity. The presence of the CD_2/PRX complex can be explained by the notion that polymerized CD tends to cluster, enabling two CDs to form a complex with one PRX molecule. The observation of the CD_2/PRX complex was exclusively noted through single X-ray diffraction analysis in the Aree (2022) research during the crystallization of the concentrated CD-PRX solution.[104] The conformational flexibility of PRX is crucial in this context, as the drug can exist in various structural forms.

Overall, the ITC results provide insights into the thermodynamics of the paroxetine-cyclodextrin binding interaction, highlighting the exothermic nature of the process and demonstrating the consistency of the binding constant determination with DOSY and Job plot.

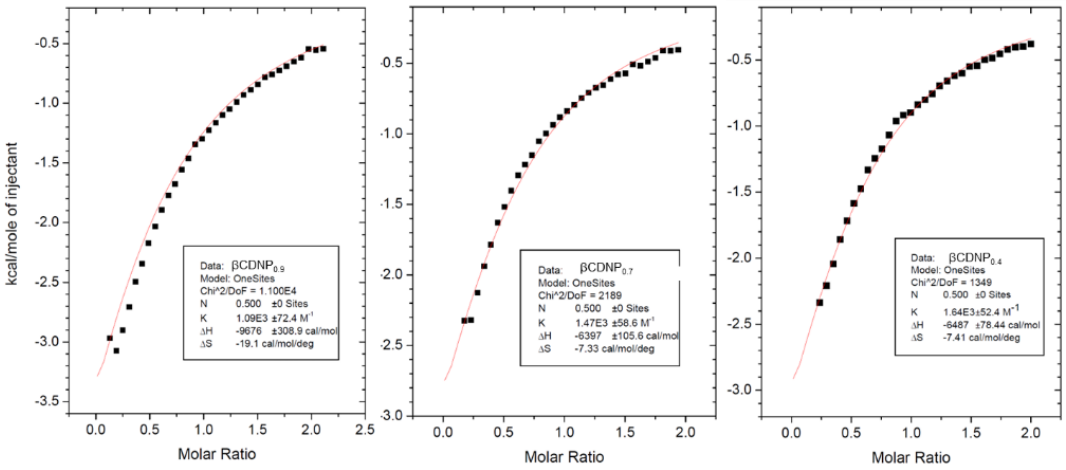

Figure 3-7. ITC binding isotherm fitted to the raw data for the interaction of PRX with $\beta CDNP_{0.9}$, $\beta CDNP_{0.7}$, $\beta CDNP_{0.4}$. Datapoints are the integrals of ITC raw data, and the lines are fitted with Origin using one-binding site models.

3-4. Discussion

Multiple methods were employed to determine the binding constants for the interaction between paroxetine and cyclodextrin. Table 3-4 shows the values of binding constants of βCD-PRX and $\beta CDNP_{2.7}$-PRX obtained by different methods.

Table 3-4. Summary of binding constants obtained by different methods.

	Binding constant $K_{1:1}$ (M^{-1})		
	DOSY-NMR	Job plot	ITC
βCD-PRX	1800	2000	1800
$\beta CDNP_{2.7}$-PRX	9010	3000	-

DOSY-NMR enables the determination of binding constants based on molecular size and interactions. DOSY-NMR measures the diffusion coefficients of molecules by averaging the diffusion coefficient of all protons. The advantages of DOSY-NMR, including non-destructive and real-time measurements, make it a valuable tool for studying molecular interactions. In contrast, Job plot offers a simpler approach by focusing on the change in chemical shift of a single proton's chemical shift. Although it offers a simpler approach, it does not provide as detailed information as DOSY-NMR. On the other hand, ITC provides a more comprehensive understanding of the thermodynamics governing the interaction between paroxetine and cyclodextrin.

Furthermore, the determined binding constants indicate the enhanced binding affinity between PRX and CDNP, with CDNP exhibiting a stronger interaction. The binding constants obtained from different methods provide complementary insights into the binding behavior of PRX with cyclodextrin as well as CDNP. Noteworthy, the 2:1 β-CD-PRX inclusion complex was observed within the polymer. In this type of complex, the PRX molecules typically adopt specific conformations to fit within the βCD cavities as observed in ROESY spectra. The 2:1 β-CD-PRX inclusion complex holds potential applications in drug delivery and pharmaceutical formulations, as it can enhance the solubility and stability of

PRX, which is especially important for the formulation of poorly water-soluble drugs like PRX. The encapsulation of the drug within the βCD cavities can protect it from environmental factors and influence its release kinetics in the body.

These findings contribute to the understanding of the host-guest interactions between cyclodextrins and paroxetine, holding implications for improving therapeutic efficacy and enhancing patient outcomes. The study of such inclusion complexes is valuable in the field of supramolecular chemistry and pharmaceutical sciences, as it helps researchers understand the behavior of drugs in different formulations and their interactions with carrier molecules like cyclodextrins. These insights hold the promise of advancing the development of more effective drug delivery systems and therapies.

3-5. Conclusion

In conclusion, the findings highlight the significance of cyclodextrin and its polymerized form in binding paroxetine. ITC and DOSY-NMR emerge as the preferred methods for accurate determination of binding constants, providing valuable insights into molecular interactions. This study contributes to a better understanding of the thermodynamics and binding behavior of paroxetine with cyclodextrin and CDNP, offering potential applications in drug delivery and pharmaceutical formulations. Moreover, the findings of this study contribute to advancing drug delivery systems and optimizing the therapeutic efficacy of paroxetine, opening new possibilities for personalized medicine in the treatment of depression and related disorders.

Chapter 4. Reduced nephrotoxicity of epichlorohydrin crosslinked β-cyclodextrin nanoparticles (βCDNPs)

4-1. Introduction

In the dynamic and rapidly evolving field of nanomedicine, the development of innovative drug delivery systems (DDS) is essential for overcoming the limitations of conventional drugs. Approximately 60% of marketed drugs incorporate hydrophobic molecules as their active components, and around 90% of drugs currently in development consist of hydrophobic compounds.[115, 116] This hydrophobicity significantly reduces the bioavailability of drugs, which is the extent and rate at which an active drug ingredient is absorbed and becomes available at the targeted site. The good bioavailability of drugs is a critical aspect of drug formulation.[117] To enhance bioavailability, various delivery systems, such as nanoparticles, liposomes, and emulsions, are utilized to improve the solubility of these hydrophobic drugs.[115-117] Among these, cyclodextrins (CDs) has emerged as a promising component in nanoparticle development for DDS. CD-conjugated nanoparticles substantially increase water solubility and drug loading capacity.[118] In comparison to other nanocarriers, like polymeric micelles and liposomes, cyclodextrin-based nanoparticles (CDNPs) provide an improved stability in biological environments. For example, in our previous paper, Oka et al. demonstrated the surprisingly extended blood circulation time of a CD-based nanoparticle.[119] This increased stability is beneficial for the controlled and sustained release of drugs, thus enhancing the efficacy of the drug delivery system. McNeil et al demonstrated how particle size, surface charge, and hydrophobicity impact the biocompatibility of nanoparticles.[120] Nanoparticles smaller than 10 nm can be readily cleared through renal or biliary pathways, while those larger than 200-300 nm can be captured by the liver, spleen, and other biological filtering systems. Additionally, the hydrophilic nature of the particle surface is crucial for evading opsonization.[121] Considering these aspects, CD-conjugated nanoparticles hold significant potential for future developments in DDS.

Building upon the preceding studies, this paper discusses the biotoxicity of βCDNPs. It has been observed that CDs can be nephrotoxic when administered parenterally.[122, 123] This nephrotoxicity is attributed to CDs, particularly βCD, which can form insoluble complexes with molecules like cholesterol, leading to their deposition and accumulation in the kidneys. Such accumulation may result in physical blockages or induce stress on renal cells.[123] To reduce this nephrotoxic potential, sulfobutylether-β-cyclodextrin (SBE-CD) has been developed as a chemically modified derivative of βCD.[124] The sulfonyl groups attached to SBE-CD increase its solubility, presumably preventing the formation of insoluble complexes with cholesterol and other hydrophobic compounds. Studies have shown that SBE-CD does not tend to accumulate in renal epithelial cells, supporting its enhanced safety profile. SBE-CD has been extensively evaluated for safety and is included in several FDA-approved pharmaceutical products.[125] Among its applications, SBE-CD has been used to improve the solubility of remdesivir, an FDA-approved treatment for certain COVID-19 patients. Further research details its use in pediatric patients, particularly focusing on the quantification of SBE-CD in human plasma.[126] One of the main aims of this paper is to present the safety of βCDNP, potentially paralleling the established safety profile of SBE-CD.

4-2. Experimental

4-2-1. Materials

β-cyclodextrin (βCD), epichlorohydrin (ECH) and Triton X-100 (purity > 99%) were purchased from Tokyo Chemical Industry Co. (Tokyo, Japan). All the chemicals were used without further purification. Cayman's creatinine (serum) colorimetric assay was provided by Cayman Chemical, USA. Arbor assays kit was purchased from Arbor Assays, USA.

4-2-2. Synthesis of cyclodextrin-based nanoparticles (CDNPs)

Conventional method

To synthesize βCDNPs, 2 g of βCD dissolved in 6.4 mL 33 wt% NaOH was stirred until complete dissolution. ECH was added, and the mixture was stirred at 30 °C using a homogenizer (POLY-TRON® PT1300D; Kinematica AG) for 6 hours. The reaction was terminated with acetone, and the product was precipitated. After removing residual ECH, the precipitate was dispersed in water, neutralized with 12 N aqueous HCl, and purified by 2-day dialysis (molecular weight cutoff of 3500). Reprecipitation eliminated insoluble components, leaving a supernatant assumed to contain βCDNPs, which was freeze-dried. βCDNP_1 to βCDNP_3 were polymerized in a previous study [40], while βCDNP_4 was newly synthesized.

Surfactant method

A total of 0.5 g of βCD was dissolved in 0.8ml of 33 wt% NaOH solution. Then, 0.8ml of 0.72 mM Triton X-100 was added and stirred for 5 min. The mixture was heated to 30 °C while vigorously stirred at 400 rpm using a homogenizer for 24 hours. Subsequent steps mirrored the conventional method. The obtained polymer was denoted as βCDNP_t.

The weight-averaged molecular weight (M_w) was determined using static light scattering coupled with gel chromatography, and hydrodynamic radius (R_h) was measured via dynamic light scattering, following procedures detailed in our

previous paper. [40] The βCD content in βCDNPs was determined by the phenol sulfuric acid method.[40]

4-2-3. In vivo experimental

All animal procedures were performed following the Guidelines for Care and Use of Laboratory Animals of the University of Kitakyushu and approved by the Animal Ethics Committee of the University of Kitakyushu. In this in vivo experiment, a total of five mice per group were utilized, employing BALB/C male mice aged seven weeks, average weight. The experimental samples, including βCD, βCDNP_4, and βCDNP_t, were prepared with dosing concentrations ranging from 3.96×10^{19} to 7.93×10^{19} number of βCD per kilogram. To determine the doses of βCDNP_4, and βCDNP_t, the doses of βCD were initially established, and the corresponding quantities of βCD were calculated accordingly. These samples were dissolved in 150 ml of 1X PBS. The samples were administered via intravenous tail injection (150 ml of the prepared sample solution). The viability and well-being of the mice were monitored, and the number of surviving mice was assessed two days after the administration.

The blood creatinine level and BUN concentrations in serum were measured in five mice at the highest dose of βCD and βCDNP_4 (7.93×10^{19} βCD/kg) and in three mice for the negative control of PBS. The blood creatinine levels were measured by using Cayman's creatinine (serum) colorimetric assay provided by Cayman Chemical, USA. The BUN concentrations were measured by using Arbor assays kit provided by Arbor Assays, USA. The absorbances were measured using iMark™ Microplate Absorbance Reader by BIO-RAD, Japan.

4-2-4. Absolute lethal LD50 of βCD

The determination of the absolute LD50 of βCD was conducted utilizing GraphPad Prism version 10.0.1 for MacOS. The least squares fit methodology was employed to model the relationship between dose concentration and the absolute LD50 values.

4-3. Results and discussion

4-3-1. Properties of β-cyclodextrin based nanoparticles (βCDNPs)

Table 4-1 presents molecular characteristics on five βCDNPs synthesized in the study, providing their feeding weight ratio, molecular weight (M_w), hydrodynamic radius (R_h), the number of cyclodextrin molecules (N_{CD}), and the weight percentage of cyclodextrin (*wt%* CD). βCDNP_4 was synthesized using a method reported previously.[33] As illustrated in Figure 1A, under a basic condition (pH = 13), the hydroxyl groups of βCD are activated and react with carbon 1 or carbon 3 of epichlorohydrin (ECH). When carbon 1 is nucleophilically attacked, a new OH group is formed, allowing the reaction to proceed, and resulting in the formation of a hyperbranched polymer that includes βCD. This mechanism indicates that the ECH to βCD feeding weight ratio is a crucial factor in controlling the molecular weight and particle size. The polymerization of βCD with ECH is highly dependent on the mixing rate during the reaction, and since the insoluble components are removed by filtration, there is variability in the sample composition, specifically in the dissolved components.[33, 40, 64] In contrast, the addition of a surfactant as a phase transfer catalyst avoids the production of insoluble components during the reaction, leading to more reproducibility in molecular characteristics.[127]

Table 4-1. Sample code and particle properties of βCDNPs.

	Sample code	Feeding weight ratio[f]	M_w (g/mol)	R_h (nm)	N_{CD}	*wt%* CD (%)
Conventional method	βCDNP_4[e]	4.25	2.64×10^5	13.4	87	37.4
With surfactant	βCDNP_t[e]	3.16	1.38×10^5	47.2	90	87.7

A polymer denoted as βCDNP_t was synthesized using a surfactant (Triton X-100) for in vivo experiments.[127, 128] It is important to note that the surfactant, specifically Triton X-100, was not directly involved in the polymerization process but played a crucial role in the synthesis of βCDNP_t. As indicated in previous studies,[127, 128] these surfactants self-assemble into clusters during the

polymerization process, facilitating the efficient transfer of ECH from the oil phase to the water phase. This phenomenon results in a homogeneous reaction solution, promoting more effective polymerization of βCD with ECH. Consequently, the nanoparticles produced using this method are expected to be larger than those obtained through previous nanoparticle synthesis approaches. βCDNP_t stands out with a notably high weight percentage of cyclodextrin (87.7%) and a large hydrodynamic radius (47.2 nm), indicating the distinct composition of this nanoparticle and potential applications.

4-3-2. Changes in particle size upon complexation with cholesterol

Figure 4-1 illustrates how the size distribution changes when βCD or βCDNP_t is mixed with cholesterol. For βCD, the particle size dramatically increases upon the addition of cholesterol, ranging from approximately 1 nm to between 100 and 500 nm. In contrast, the size of βCDNP_t does not change significantly. The

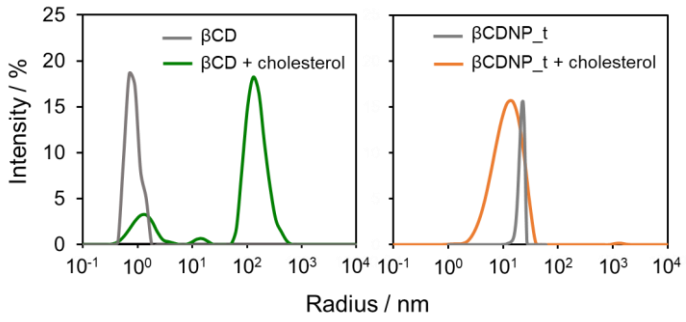

Figure 4-1. Intensity-based size distribution histograms obtained by DLS for βCD or βCDNP_t and cholesterol mixtures.

particle size slightly decreased for βCDNP_t + cholesterol, as indicated by the intensity versus radius plot. However, upon examining the original correlation function of DLS, the two samples exhibited almost identical curves. Therefore, we assume that there is no substantial difference between the two samples. On the other hand, there was an unmistakable significant difference in the case of βCD. According to structural studies of the βCD/cholesterol complex, long molecules such as cholesterol can connect two βCDs.[129, 130] This interaction seems to be the reason for the formation of aggregates in water for βCD/cholesterol complexes. In the case of βCDNP_t, the βCD molecules are immobilized by cross-linkers, preventing them from moving to form dimers.

Additionally, the surface of βCDNP_t is likely covered with water-soluble CDs, providing water solubility to βCDNP_t. These characteristics contribute to the prevention of aggregate formation. As mentioned earlier in the introduction, the formation of larger aggregates, as observed in βCD/cholesterol complexes, is a primary cause of βCD's nephrotoxicity. In contrast, βCDNP_t, with its reduced tendency to form aggregates, appears to offer a significant advantage in mitigating this risk.

4-3-3. Survival analysis at various dosing concentrations

Figure 4-2 shows the survival ratio of mice as the doses of βCD, βCDNP_t, βCDNP_4 are increased. Note that the dose is expressed as the number of βCD molecules per unit weight of the mouse, allowing for a direct comparison between βCD and βCDNPs on the same basis.

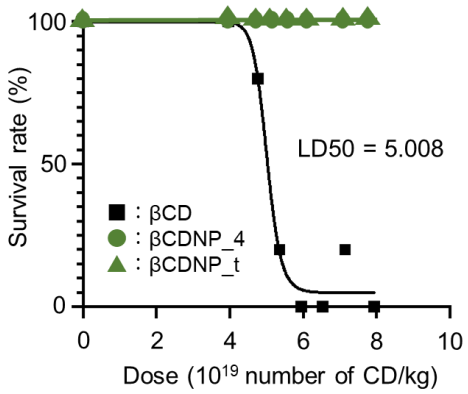

Figure 4-2. Survival dependency on βCD dose concentrations of βCD, βCDNP_t, and βCDNP_4.

For βCD, all mice survived at the lowest dose (3.96×10^{19} βCD/kg equivalent to 88.4 mg βCD/kg in terms of βCD weight. The same applies to the doses below). However, as the dose increased, the survival ratio decreased, and all mice failed to survive at doses exceeding 6×10^{19} βCD/kg (134 mg βCD/kg). Based on this curve, the LD50 (lethal dose for 50% of the population) of βCD was estimated to be 5.0×10^{19} βCD/kg (111.7 mg βCD/kg). In contrast, for both βCDNP_4 and βCDNP_t, even at the highest dose of 7.93×10^{19} βCD/kg (150 mg βCD/kg), all mice remained in excellent health, as indicated by both creatinine and blood urea nitrogen (BUN) levels in the blood, as shown in Table 4-2. Here, kidney health

levels were evaluated by assessing creatinine and BUN concentrations at the highest βCDNP dose, compared to a negative control of PBS. The reference range for creatinine and BUN for C57BL/6 mice is 0.2 - 0.7 mg/dl and 18-35 mg/dl, respectively.[131] Blood creatinine levels can be used to assess kidney function, and elevated levels may suggest acute or chronic kidney disorders. BUN is also a measure of kidney health. Although we could not find previous studies on the LD50 of intravenous administration for mice, the LD50 of βCD for intraperitoneal and subcutaneous routes in rodent males are 372.03 and 419.4 mg/kg, respectively.[92] The current LD50 result (134 mg/kg) for βCD seems a reasonable value, considering the difference in administration routes and the use of mice. It is remarkable that βCDNPs exhibited consistent and complete survival across all administered doses, suggesting a high degree of biocompatibility and minimal toxicity at the tested concentrations. These findings collectively underscore the robust safety profiles of βCDNP_4 and βCDNP_t, positioning them as good candidates for biomedical applications. As shown in Figure 2, βCDNP_t does not form large aggregates even after ingesting cholesterol. This non-aggregating ability could reduce the toxicity of βCDNPs, which may be the reason for the observed results.

Table 4-2. Creatinine and blood urea nitrogen (BUN) levels in the serum at the highest dose of βCD and βCDNP_4 (7.93×10^{19} βCD/kg) and in the negative control of PBS.

Sample	Creatinine (mg/dl)	BUN (mg/dl)
1×PBS (N:3)	0.16 ±0.05	12±0.8
βCD (N:5)	0.21	16
βCDNP_4 (N:5)	0.25±0.1	14±0.5

4-4. Conclusion

The present study focuses on developing and characterizing cyclodextrin-based nanoparticles (CDNPs) for enhancing drug delivery of hydrophobic drugs. Key findings include the successful synthesis of βCDNPs and their characterization. The study explored the biocompatibility and safety of βCDNPs, revealing a reduced tendency to form aggregates with cholesterol and a high degree of biocompatibility in survival analyses with mice, suggesting a lower risk of nephrotoxicity. These findings position βCDNPs as promising candidates for efficient and safe drug delivery systems, especially for hydrophobic pharmaceuticals.

Chapter 5. Advantages and limitations of utilizing diffusion ordered NMR spectroscopy (DOSY) in determining binding constant of cyclodextrin nanoparticles (CDNPs)

In our previous study, we determined the enhanced binding constant of CDNPs with MGS using the phase solubility method.[33, 132] We examined the enhanced binding for βCDNP_1 as shown in Figure 5-1, confirming that the nanoparticulation of βCD by ECH increased the binding constant by a factor of nearly 100. Here, MGS and CDs form a 1:1 stoichiometric complex. In this case, the total MGS concentration (S_{total}) in aqueous solutions can be given by Eq. 1 using a given total of cyclodextrin in aqueous solution $[\mathrm{CD}]_{\mathrm{t}}$ ($\equiv$ [MGS⁄CD] + [CD]) and the intrinsic solubility of MGS: S_0 (i.e., the solubility in aqueous medium when no CD is present):

$$S_{\mathrm{total}} = S_0 + \frac{K\,S_0}{1 + K\,S_0}[\mathrm{CD}]_{\mathrm{t}} \tag{14}$$

Here, K is the binding constant between CD and MGS. The values of S_{total} and $[\mathrm{CD}]_{\mathrm{t}}$ are determined experimentally by UV measurements and the phenol sulfuric acid method [33, 40], respectively, and both K and S_0 are constant values for a given solution conditions such as temperature and pH. Therefore, Eq. 14 shows that, when S_{total} is plotted against $[\mathrm{CD}]_{\mathrm{t}}$, the plot should constitute a straight line, and from the slope and intercept we can determine K. As shown in Figure 5-1, the data points for both βCD and βCDNP_1 fit a straight line and the determined K values are shown in the figure. While the phase solubility method is ideal for determining 1:1 binding when the guest molecule has exceptionally

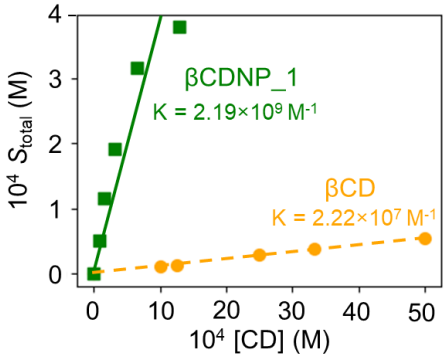

Figure 5-1. S_{total} vs. [CD] plot of βCDNP_1-MGS (green) and βCD-MGS (orange).

low solubility such as MGS, we found that it is not the preferred method for more soluble compounds than MGS, such as vanillin or PRX (although they are still hydrophobic). This is due to excessive sample dilution, which can lead to significant errors. In such cases, NMR and ITC emerge as superior choices. For NMR, the binding constant for them can be determined through techniques like DOSY-NMR or the Job plot method.[40] Ideally, the guest compound should have a solubility higher than 2mM, preferably above 5mM, for more accurate NMR measurements. This is because having a sufficiently high concentration of the sample (in this case, the guest compound) is important for achieving a strong signal of NMR.

Figure 5-2 illustrates 2D DOSY-NMR comparisons between βCD-PRX (Figure 5A) and βCDNP_2-PRX (Figure 5-2B), as well as βCD-vanillin (Figure 5-2C) and βCDNP_2-vanillin (Figure 5-2D), as reported in a previous study. [40, 133] According to the 1:1 model, the binding constant for βCD-PRX is 1800 M^{-1}, while for βCDNP_2-PRX, it significantly increases to 9200 M^{-1}. [133] Similarly, for vanillin, the binding constant for βCD-vanillin is 55 M^{-1}, whereas for βCDNP_2-vanillin, it remarkably rises to 6800 M^{-1}. DOSY-NMR offers several advantages in determining binding constants in molecular interactions. Firstly, it provides valuable information about the size and diffusion properties of different molecular species in a mixture, enabling the differentiation between free and bound ligands. This technique is particularly advantageous for studying host-guest interactions, as it allows for direct observation of changes in molecular diffusion rates upon complex formation. Moreover, DOSY-NMR does not require the introduction of external agents or labels, preserving the native state of the interacting molecules. Its ability to operate in solution makes it suitable for studying dynamic systems and capturing information about binding constants under physiologically relevant conditions. Additionally, DOSY-NMR can be applied to samples with varying concentrations, offering versatility in experimental setups.

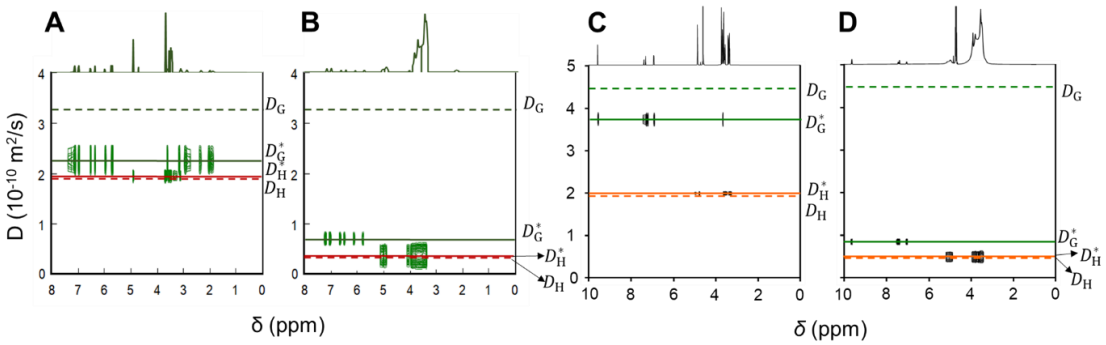

Figure 5-2. 2D DOSY-NMR comparing A: βCD-PRX and B: βCDNP_2-PRX. 2D DOSY-NMR comparing C: βCD-vanillin and D: βCDNP_2-vanillin.

Despite its merits, DOSY-NMR also presents certain limitations when employed to determine binding constants. A notable drawback is the assumption of a 1:1 binding stoichiometry, which may not accurately represent more complex interactions involving different stoichiometries. Additionally, the technique relies on the separation of signals based on molecular diffusion rates, and in cases where multiple species have similar diffusion coefficients, discerning distinct contributions can be challenging. DOSY-NMR is also sensitive to changes in temperature and viscosity, which may impact the accuracy and reproducibility of results. Furthermore, the method requires careful consideration of experimental conditions, such as the choice of solvent and the concentration of the interacting species, to ensure optimal performance. Despite these limitations, when used judiciously and in conjunction with complementary techniques, DOSY-NMR remains a valuable tool for studying molecular interactions and determining binding constants in diverse systems, contributing valuable insights into molecular recognition processes.

Chapter 6. Summary and conclusion

In summary, this thesis delved into the intricate realm of cyclodextrin-based nanoparticles (CDNPs) and their interactions with guest molecules, focusing on vanillin and paroxetine hydrochloride hemihydrate (PRX). Through the utilization of advanced analytical techniques, particularly diffusion-ordered NMR spectroscopy (DOSY-NMR) alongside other methods, the study aimed to achieve several objectives. Firstly, it aimed to determine the binding constants between CDNPs and PRX accurately, shedding light on the strength and thermodynamic parameters of the interactions. Secondly, it sought to explore the molecular mechanisms underlying CDNP-drug interactions, unraveling the structural features and binding modes driving the formation of complexes. Additionally, the study aimed to compare the effectiveness of CDNPs with native cyclodextrins in enhancing drug solubility and stability. Lastly, it aimed to assess the biotoxicity of βCDNPs and evaluate their potential safety profile. Through rigorous experimentation and analysis, the thesis aimed to contribute to a deeper understanding of CDNP-drug interactions, their potential as drug delivery systems, and their safety profile, thereby advancing their development and application in biomedicine.

In conclusion, this thesis significantly advances our understanding of cyclodextrin-based nanoparticles (CDNPs) and their potential in drug delivery applications. Through comprehensive investigations, the study elucidated the binding constants between CDNPs and hydrophobic compounds such as vanillin paroxetine hydrochloride (PRX), shedding light on the thermodynamics and stability of CDNP-drug complexes. Importantly, the study underscored the value of diffusion-ordered NMR spectroscopy (DOSY-NMR) as a powerful and versatile tool for accurately determining the binding constants of CDNPs with guest molecules. DOSY-NMR provided direct insights into the molecular interactions within host-guest complexes, facilitating the quantification of binding affinities and offering valuable information on complex formation dynamics. Furthermore, the study uncovered the molecular mechanisms

underlying CDNP-drug interactions, providing valuable insights into their structural features and binding modes. Additionally, by comparing the effectiveness of CDNPs with native cyclodextrins and evaluating their biotoxicity profile, the thesis addressed critical aspects of CDNPs translational potential in biomedical applications. Overall, the findings contribute to the advancement of cyclodextrin-based drug delivery systems, offering promising avenues for the development of targeted and efficacious therapeutics.

Appendix A

CDNP characterization of physical properties

Determination of the weight average molecular weight (M_w) and hydrodynamic radius (R_h)

Size exclusion chromatography coupled with multiangle light scattering (SEC-MALS) and others SEC-MALS measurements were carried out for the CDNPs using a Shodex column (SB802.5 and SB806) at 40 °C with 10 mM aqueous NaCl as the eluent to measure M_w. We prepared a sample solution of 1 mg/mL in 10 mM aqueous solution. The solution was optically purified with a PTFE (Polytetrafluoroethylene) membrane with 0.2 μm pores and injected into the column. The output from the column was passed sequentially through an MALS detector (Wyatt Technology, Dawn Heleos II, wavelength: λ = 658 nm) and an RI detector (Wyatt Technology, 1.2 – 1.8 RIU, wavelength: λ = 488 – 690 nm). The specific refractive index increments (∂n/∂c) of the CDNPs in 10mM aqueous NaCl was determined by a differential refractometer (Otsuka Electronics DRM-1020, wavelength: λ = 633 nm). Data acquisition and molecular weight calculation were performed using the ASTRA software, version 7.3.2 (Wyatt Technology).

The DLS measurement was operated using the facility of DelsaMax Pro (Beckman Coulter, Inc.) to determine the hydrodynamic radius R_h. We prepared a sample solution of 10 mg/mL in aqueous solution.

The typical example of GPC chromatogram and the angular dependence of static light scattering to determine M_w is shown in the Figure A-1A. The distribution of R_h was unimodal as shown in the Figure A-1B.

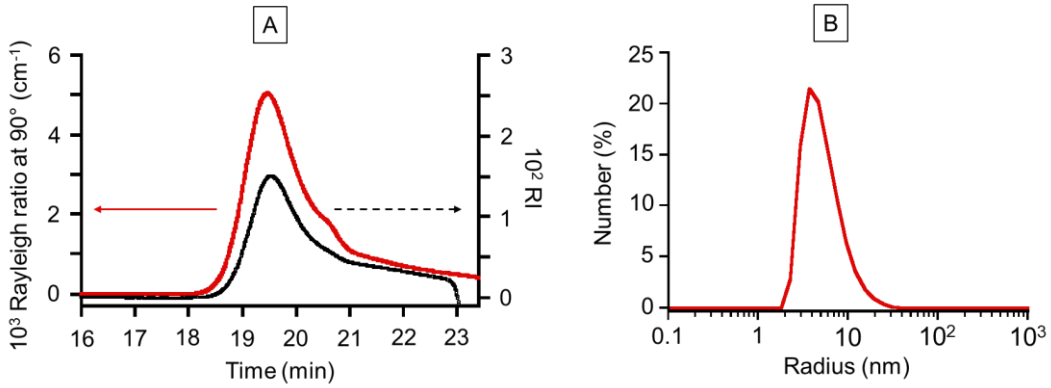

Figure A-1. A: SEC-MALS fractogram of βCDNP$_{2.7}$; B: Number size distribution of βCDNP2.7in water

Determination of the carbohydrate concentration in CDNPs

The CD weight percent in CDNPs was determined by the phenol sulfuric acid method. Dried CDNP (0.025 g) was refluxed at 100 °C for 8 h in 0.5M H_2SO_4 (15 mL) to break down the reacted CD to a pentose. Then, the solution was reacted with 5% (w/w) phenol and concentrated H_2SO_4. The final product was brown-orange in color, and the absorbance was detected by a UV–Vis spectrophotometer (Jasco, V-630) at 488 nm. The absorbance was converted into the CD weight percent (*wt%* CD) by use of a calibration curve established with glucose D(+). Here, we confirmed that polymerized ECH with poly vinyl alcohol samples did not show any absorbance after we treated them in the same manner. From the CD weight percent and M_w of CDNP, we calculated the number of CDs in one CDNP particle (N_{CD}).

NMR of βCDNP in DMSO

We carried out ^{1}H-NMR spectra of $\beta CDNP_{0.9}$ in DMSO and its results showed disappearance of all -OH peaks in as shown in Figure A-2.

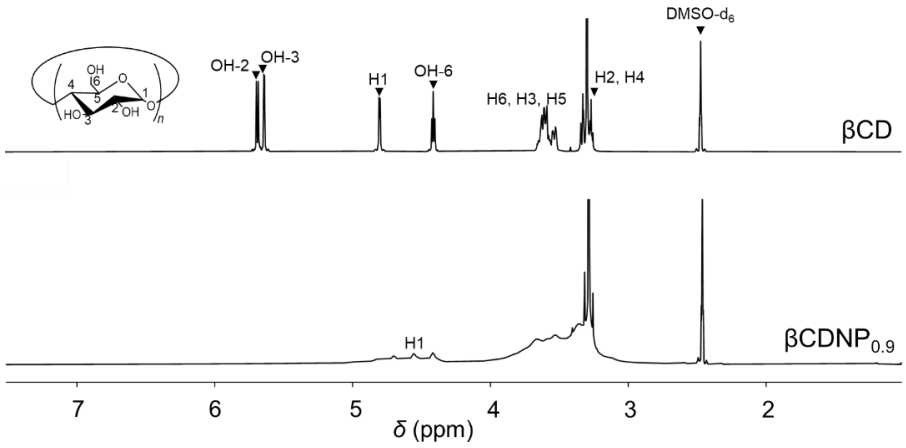

Figure A-2. ^{1}H-NMR spectra of βCD and $\beta CDNP_{0.9}$ in DMSO

Continuous variation method (Job plot) by NMR

When the host-guest complexation equilibrium has a very fast exchange rate compared with the NMR time scale. The observed chemical shift of guest appears at the weighted average chemical shift of the free guest and complexed guest:

$$aH + bG \leftrightarrow H_aG_b$$

$$\delta_{G\_obs} = \delta_G.(1-x) + \delta_{HG}.x \qquad (a.1)$$

Here δ_{G_obs}, δ_G and δ_{HG} are observed chemical shift of guest, chemical shift of free and complexed guest, respectively. x is ratio of complexed guest at equilibrium [HG] over total guest $[G]_i$.

$$x = \frac{b[HG]}{[G]_i} \qquad (a.2)$$

Substitution of equation (a.2) into equation (a.1) result in the expression:

$$[G]_i.\Delta\delta_G = b.[HG].(\delta_{HG} - \delta_G) \text{ with } \Delta\delta_G = (\delta_{G\_obs} - \delta_G) \qquad (a.3)$$

Equation (a.3) means that $[G]_i.\Delta\delta_G$ is proportional to [HG], since $b.(\delta_{HG} - \delta_G)$ is constant. Consequently, the stoichiometry is obtained from the x-coordinate at the maximum in the modified Job's plot, where $[G]_i.\Delta\delta_G$ is plotted as y-

coordinate and x axis is r = $[G]_i/([H]_i+[G]_i)$. The maximum value for $[G]_i.\Delta\delta_G$ will occur at $r = b/(a+b)$, where a and b are, the proportions of CD and vanillin in the complex, respectively. For instance, if the stoichiometry of the complex is 1:1 ($a = b = 1$), the maximum value for the examined parameter will be reached at $r = 0.5$

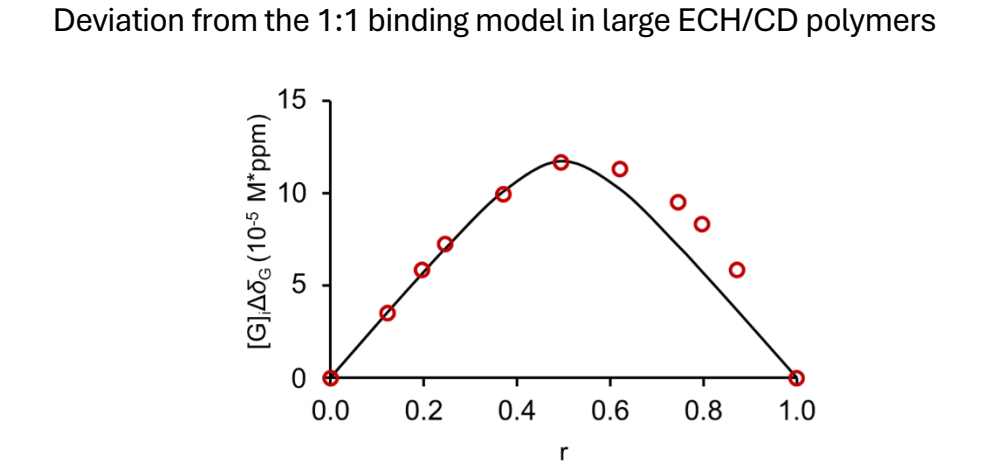

Figure A-3. Job plot for vanillin and βCDNP2.7in D_2O at 25 °C. The total concentration ($[G]_i+[H]_i$) was fixed at 4.9 mM.

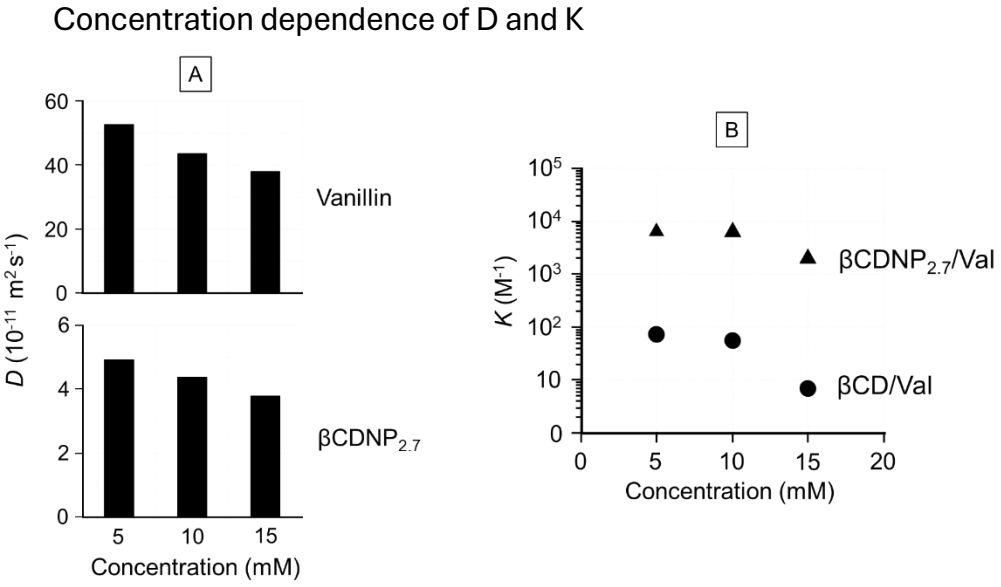

Figure A-4. A: Concentration dependence of diffusion coefficient of vanillin and $\beta CDNP_{2.7}$; B: Concentration dependence of binding constant of CD and βCDNP2.7to vanillin.

Complex formation ability of CDNP and DXNP

An amount of vanillin (3.35 mg) was added into the βCDNP$_{0.9}$ or DXNP solution (1ml, 50 mg/mL). The mixture was stirred in 1 day at room temperature. After centrifugation (12000 rpm for 5 min), the upper solution was collected and purified by spin dialysis (cut-off M_w = 3500 g/mol). The solution containing only complex finally was filtered before measuring UV-vis. The absorbance of vanillin was detected by UV-vis spectrophotometer.

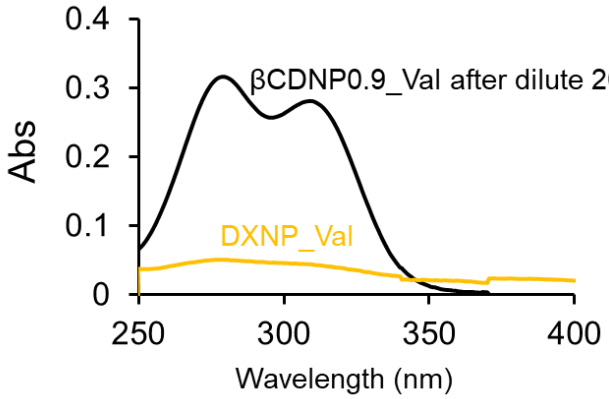

Figure A-5. The UV-vis spectra of the βCDNP$_{0.9}$-Val and DXNP-Val complex.

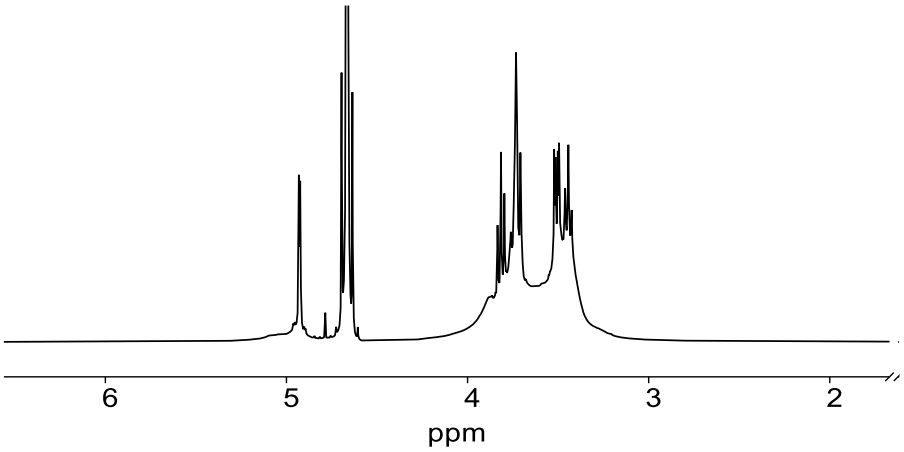

Figure A-6. The ^{1}H-NMR spectra of mixture βCDNP$_{0.9}$/βCD at 10mM, 20°C in D_2O

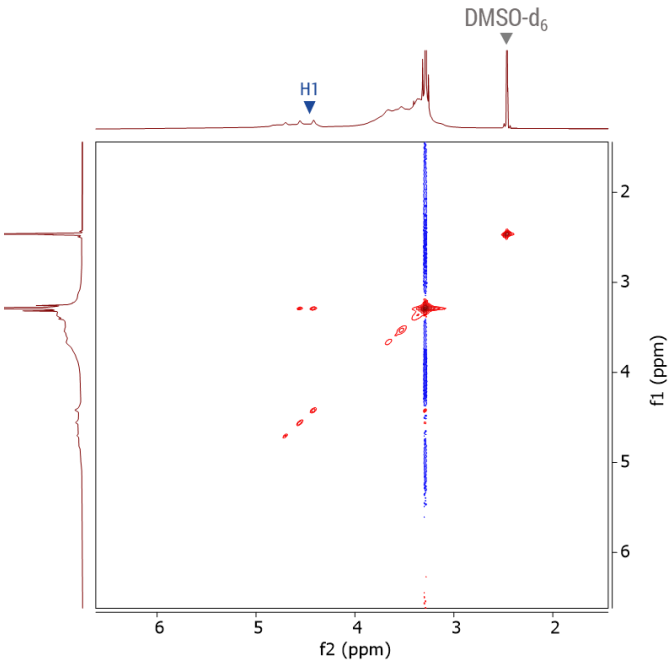

Figure A-7. The NOESY spectra of βCDNP$_{0.9}$ in DMSO-d$_6$, 25°C

Appendix B

Table B- 1. Sample code and particle properties of βCDNPs

Sample code	Feeding weight ratio[c]	M_w (g/mol)	R_h (nm)	N_{CD}	*wt%* CD (%)
βCDNP_1[a]	4.25	1.44×10^4	5.4	65	50.9
βCDNP_2[b]	4.25	7.29×10^4	3.5	17	26.7

a: phase solubility method

b: DOSY method

c: feeding weight ratio of ECH to CD

References

1. Van, D. T. H.; Anh, D. T. N.; Fujii, S.; Sakurai, K., Enhanced binding constant of cyclodextrin to alpha-mangostin in hyperbranched polymers. *Chem. Lett.* **2020,** *49* (10), 1144-1146.

2. Hedges, A., Chapter 22 - Cyclodextrins: Properties and Applications. In *Starch (Third Edition)*, BeMiller, J.; Whistler, R., Eds. Academic Press: San Diego, 2009; pp 833-851.

3. Esteso, M. A.; Romero, C. M., Cyclodextrins: Properties and Applications. *Int J Mol Sci* **2024,** *25* (8), 4547.

4. Tiwari, G.; Tiwari, R.; Rai, A. K., Cyclodextrins in delivery systems: Applications. *J. Pharm. Bioallied Sci.* **2010,** *2* (2), 72-79.

5. Li, J.; Xu, F.; Dai, Y.; Zhang, J.; Shi, Y.; Lai, D.; Sriboonvorakul, N.; Hu, J., A Review of Cyclodextrin Encapsulation and Intelligent Response for the Release of Curcumin. *Polymers* **2022,** *14* (24), 5421.

6. Carneiro, S. B.; Costa Duarte, F.; Heimfarth, L.; Siqueira Quintans, J. S.; Quintans-Júnior, L. J.; Veiga Júnior, V. F. D.; Neves de Lima Á, A., Cyclodextrin⁻Drug Inclusion Complexes: In Vivo and In Vitro Approaches. *Int J Mol Sci* **2019,** *20* (3).

7. Ferreira, L.; Mascarenhas-Melo, F.; Rabaça, S.; Mathur, A.; Sharma, A.; Giram, P. S.; Pawar, K. D.; Rahdar, A.; Raza, F.; Veiga, F.; Mazzola, P. G.; Paiva-Santos, A. C., Cyclodextrin-based dermatological formulations: Dermopharmaceutical and cosmetic applications. *Colloids Surf. B Biointerfaces.* **2023,** *221*, 113012.

8. Kfoury, M.; Hădărugă, D.; Hădărugă, N.; Fourmentin, S., Cyclodextrins as encapsulation material for flavors and aroma. In *Encapsulations*, Alexandru, M. G., Ed. Elsevier 2016; pp 127-192.

9. Xiao, Z.; Zhang, Y.; Niu, Y.; Ke, Q.; Kou, X., Cyclodextrins as carriers for volatile aroma compounds: A review. *Carbohydrate Polymers* **2021,** *269*, 118292.

10. Christaki, S.; Spanidi, E.; Panagiotidou, E.; Athanasopoulou, S.; Kyriakoudi, A.; Mourtzinos, I.; Gardikis, K., Cyclodextrins for the Delivery of

Bioactive Compounds from Natural Sources: Medicinal, Food and Cosmetics Applications. *Pharmaceuticals (Basel)* **2023,** *16* (9).

11. Kurek, M.; Benaida-Debbache, N.; Elez Garofulić, I.; Galić, K.; Avallone, S.; Voilley, A.; Waché, Y., Antioxidants and Bioactive Compounds in Food: Critical Review of Issues and Prospects. *Antioxidants (Basel)* **2022,** *11* (4).

12. Casanova, F.; Santos, L., Encapsulation of cosmetic active ingredients for topical application – a review. *Microencapsul.* **2016,** *33* (1), 1-17.

13. Dahabra, L.; Broadberry, G.; Le Gresley, A.; Najlah, M.; Khoder, M., Sunscreens Containing Cyclodextrin Inclusion Complexes for Enhanced Efficiency: A Strategy for Skin Cancer Prevention. *Molecules* **2021,** *26* (6).

14. Syeda, S. E. Z.; Nowacka, D.; Khan, M. S.; Skwierawska, A. M., Recent Advancements in Cyclodextrin-Based Adsorbents for the Removal of Hazardous Pollutants from Waters. *Polymers (Basel)* **2022,** *14* (12).

15. Okasha, A. T.; Abdel-Khalek, A. A.; Alenazi, N. A.; AlHammadi, A. A.; Al Zoubi, W.; Alhammadi, S.; Ko, Y. G.; Abukhadra, M. R., Progress of synthetic cyclodextrins-based materials as effective adsorbents of the common water pollutants: Comprehensive review. *J. Environ. Chem. Eng.* **2023,** *11* (3), 109824.

16. Szente, L.; Szemán, J., Cyclodextrins in Analytical Chemistry: Host–Guest Type Molecular Recognition. *Analytical Chemistry* **2013,** *85* (17), 8024-8030.

17. Sun, L.; Stenken, J. A., The effect of β-cyclodextrin on liquid chromatography/electrospray-mass spectrometry analysis of hydrophobic drug molecules. *J. Chromatogr. A.* **2007,** *1161* (1), 261-268.

18. Liu, Z.; Xu, W.; Kovaleva, E. G.; Cheng, J.; Li, H., Recent progress in encapsulation and controlled release of pesticides based on cyclodextrin derivative carriers. *Advanced Agrochem* **2022,** *1* (2), 89-99.

19. Morillo, E.; Madrid, F.; Lara-Moreno, A.; Villaverde, J., Soil bioremediation by cyclodextrins. A review. *Int. J. Pharm.* **2020,** *591*, 119943.

20. Martel, B.; Morcellet, M.; Ruffin, D.; Vinet, F.; Weltrowski, L., Capture and Controlled Release of Fragrances by CD Finished Textiles. *J. Inclusion Phenom. Macrocyclic Chem.* **2002,** *44* (1), 439-442.

21. Ghitman, J.; Voicu, S. I., Controlled drug delivery mediated by cyclodextrin-based supramolecular self-assembled carriers: From design to clinical performances. *Carbohydr. Polym. Technol. Appl.* **2023,** *5*, 100266.

22. Jansook, P.; Ogawa, N.; Loftsson, T., Cyclodextrins: structure, physicochemical properties and pharmaceutical applications. *Int. J. Pharm.* **2018,** *535* (1), 272-284.

23. Hua, S., Physiological and Pharmaceutical Considerations for Rectal Drug Formulations. *Front. Pharmacol.* **2019,** *10*, 1196.

24. Uekama, K., Design and Evaluation of Cyclodextrin-Based Drug Formulation. *Chem. Pharm. Bull.* **2004,** *52* (8), 900-915.

25. Păduraru, D. N.; Niculescu, A. G.; Bolocan, A.; Andronic, O.; Grumezescu, A. M.; Bîrlă, R., An Updated Overview of Cyclodextrin-Based Drug Delivery Systems for Cancer Therapy. *Pharmaceutics* **2022,** *14* (8).

26. Aiassa, V.; Garnero, C.; Zoppi, A.; Longhi, M. R., Cyclodextrins and Their Derivatives as Drug Stability Modifiers. *Pharmaceuticals* **2023,** *16* (8), 1074.

27. Adamkiewicz, L.; Szeleszczuk, Ł., Review of Applications of Cyclodextrins as Taste-Masking Excipients for Pharmaceutical Purposes. *Molecules* **2023,** *28* (19).

28. Conceição, J.; Adeoye, O.; Cabral-Marques, H. M.; Lobo, J. M. S., Cyclodextrins as excipients in tablet formulations. *Drug Discov. Today* **2018,** *23* (6), 1274-1284.

29. Sarabia-Vallejo, Á.; Caja, M. D. M.; Olives, A. I.; Martín, M. A.; Menéndez, J. C., Cyclodextrin Inclusion Complexes for Improved Drug Bioavailability and Activity: Synthetic and Analytical Aspects. *Pharmaceutics* **2023,** *15* (9).

30. Devi, L. S.; Casadidio, C.; Gigliobianco, M. R.; Di Martino, P.; Censi, R., Multifunctionality of cyclodextrin-based polymeric nanoparticulate delivery systems for chemotherapeutics, combination therapy, and theranostics. *Int. J. Pharm.* **2024,** *654*, 123976.

31. Gadade, D. D.; Pekamwar, S. S., Cyclodextrin Based Nanoparticles for Drug Delivery and Theranostics. *Adv. Pharm. Bull.* **2020,** *10* (2), 166-183.

32. Rout, D. R.; Jena, H. M., Synthesis of novel epichlorohydrin cross-linked β-cyclodextrin functionalized with reduced graphene oxide composite adsorbent

for treatment of phenolic wastewater. *Environ. Sci. Pollut. Res. Int.* **2022,** *29* (48), 73444-73460.

33. Doan, V. T. H.; Lee, J. H.; Takahashi, R.; Nguyen, P. T. M.; Nguyen, V. A. T.; Pham, H. T. T.; Fujii, S.; Sakurai, K., Cyclodextrin-based nanoparticles encapsulating α-mangostin and their drug release behavior: potential carriers of α-mangostin for cancer therapy. *Polym. J.* **2020,** *52* (4), 457-466.

34. Másson M, S. B., Matthíasson K, Loftsson T. , Investigation of Drug–Cyclodextrin Complexes by a Phase-Distribution Method: Some Theoretical and Practical Considerations. *Chem. Pharm. Bull.* **2005,** *53* (8), 958-964.

35. Cameron, K. S.; Fielding, L., NMR Diffusion Spectroscopy as a Measure of Host–Guest Complex Association Constants and as a Probe of Complex Size. *J. Org. Chem.* **2001,** *66* (21), 6891-6895.

36. Williamson, M. P., Using chemical shift perturbation to characterise ligand binding. *Prog. Nucl. Magn. Reson. Spectrosc.* **2013,** *73*, 1-16.

37. Palmer, A. G., 3rd, A topical issue: NMR investigations of molecular dynamics. *J. Biomol. NMR* **2009,** *45* (1-2), 1-4.

38. Krūkle-Bērziņa, K. n.; Lends, A.; Boguszewska-Czubara, A., Cyclodextrin Metal–Organic Frameworks as a Drug Delivery System for Selected Active Pharmaceutical Ingredients. *ACS Omega* **2024,** *9* (8), 8874-8884.

39. Haouas, M.; Falaise, C.; Leclerc, N.; Floquet, S.; Cadot, E., NMR spectroscopy to study cyclodextrin-based host–guest assemblies with polynuclear clusters. *Dalton Transactions* **2023,** *52* (38), 13467-13481.

40. Doan, A. T. N.; Doan, V. T. H.; Katsuki, J.; Fujii, S.; Kono, H.; Sakurai, K., Dramatically Increased Binding Constant of Water-Soluble Cyclodextrin Hyperbranched Polymers: Explored with Diffusion Ordered NMR Spectroscopy (DOSY). *ACS Omega* **2022,** *7* (13), 10890-10900.

41. Fielding, L., Determination of Association Constants (K_a) from Solution NMR Data. *Tetrahedron* **2000,** *56* (34), 6151-6170.

42. Biwer, A.; Antranikian, G.; Heinzle, E., Enzymatic production of cyclodextrins. *Appl. Microbiol. Biotechnol.* **2002,** *59*, 609-17.

43. Crini, G.; Fourmentin, S.; Fenyvesi, É.; Torri, G.; Fourmentin, M.; Morin-Crini, N., Fundamentals and Applications of Cyclodextrins. In *Cyclodextrin Fundamentals, Reactivity and Analysis*, Fourmentin, S.; Crini, G.; Lichtfouse, E., Eds. Springer International Publishing: Cham, 2018; pp 1-55.

44. Gonzalez Pereira, A.; Carpena, M.; García Oliveira, P.; Mejuto, J. C.; Prieto, M. A.; Simal Gandara, J., Main Applications of Cyclodextrins in the Food Industry as the Compounds of Choice to Form Host-Guest Complexes. *Int J Mol Sci* **2021,** *22* (3), 1339.

45. Loftsson, T.; Duchêne, D., Cyclodextrins and their pharmaceutical applications. *Int. J. Pharm.* **2007,** *329* (1), 1-11.

46. Köse, K.; Tüysüz, M.; Aksüt, D.; Uzun, L., Modification of cyclodextrin and use in environmental applications. *Environ. Sci. Pollut. Res.* **2021**, 1 - 28.

47. Fenyvesi, É.; Puskás, I.; Szente, L., Cyclodextrin-Steroid Interactions and Applications to Pharmaceuticals, Food, Biotechnology and Environment. In *Cyclodextrin Applications in Medicine, Food, Environment and Liquid Crystals*, Fourmentin, S.; Crini, G.; Lichtfouse, E., Eds. Springer International Publishing: Cham, 2018; pp 19-57.

48. Yao, X.; Huang, P.; Nie, Z., Cyclodextrin-based polymer materials: From controlled synthesis to applications. *Prog. Polym. Sci.* **2019,** *93*, 1-35.

49. Liu, Y.; Lin, T.; Cheng, C.; Wang, Q.; Lin, S.; Liu, C.; Han, X., Research Progress on Synthesis and Application of Cyclodextrin Polymers. *Molecules* **2021,** *26* (4).

50. Petitjean, M.; García-Zubiri, I. X.; Isasi, J. R., History of cyclodextrin-based polymers in food and pharmacy: a review. *Environ. Chem. Lett.* **2021,** *19* (4), 3465-3476.

51. Morin-Crini, N.; Winterton, P.; Fourmentin, S.; Wilson, L. D.; Fenyvesi, E.; Crini, G., Water-insoluble β-cyclodextrin–epichlorohydrin polymers for removal of pollutants from aqueous solutions by sorption processes using batch studies: A review of inclusion mechanisms. *Prog. Polym. Sci.* **2018,** *78*, 1-23.

52. Li, X.; Zhou, M.; Jia, J.; Ma, J.; Jia, Q., Design of a hyper-crosslinked β-cyclodextrin porous polymer for highly efficient removal toward bisphenol a from water. *Sep. Purif. Technol.* **2018,** *195*, 130-137.

53. Wang, J.; Cheng, G.; Lu, J.; Chen, H.; Zhou, Y., PDA-cross-linked beta-cyclodextrin: a novel adsorbent for the removal of BPA and cationic dyes. *Water Sci. Technol.* **2020,** *81* (11), 2337-2350.

54. Wang, J.-w.; Lan, D.; Yong-qiang, L.; Li, R.-f.; Yang, X.-t.; Lan, G.-h.; Qiu, H.-y.; Xu, B., Adsorption properties of β-cyclodextrin modified hydrogel for methylene blue. *Carbohydr. Res.* **2021,** *501*, 108276.

55. Kono, H.; Nakamura, T.; Hashimoto, H.; Shimizu, Y., Characterization, molecular dynamics, and encapsulation ability of β-cyclodextrin polymers crosslinked by polyethylene glycol. *Carbohydr. Polym.* **2015,** *128*, 11-23.

56. Zhao, D.; Zhao, L.; Zhu, C.-S.; Huang, W.-Q.; Hu, J.-L., Water-insoluble β-cyclodextrin polymer crosslinked by citric acid: synthesis and adsorption properties toward phenol and methylene blue. *J. Inclusion Phenom. Macrocyclic Chem.* **2009,** *63* (3), 195-201.

57. Sikder, M. T.; Islam, M. S.; Kikuchi, T.; Suzuki, J.; Saito, T.; Kurasaki, M., Removal of Copper Ions From Water Using Epichlorohydrin Cross-Linked β-Cyclodextrin Polymer: Characterization, Isotherms and Kinetics. *Water Environ. Res.* **2014,** *86* (4), 296-304.

58. Kitaoka, M.; Hayashi, K., Adsorption of Bisphenol A by Cross-Linked β-Cyclodextrin Polymer. *J. Inclusion Phenom. Macrocyclic Chem.* **2002,** *44* (1), 429-431.

59. Poornima, K.; Deveswaran, R.; Bharath, S.; Basavaraj, B.; Madhavan, V., Synthesis and evaluation of β-cyclodextrin-epichlorohydrin inclusion complex as a pharmaceutical excipient. *J. Fundam. Appl. Sci.* **2015,** *7* (2), 203-221.

60. Gidwani, B.; Vyas, A., Synthesis, characterization and application of epichlorohydrin-β-cyclodextrin polymer. *Colloids Surf., B* **2014,** *114*, 130-7.

61. Szeman, J.; Ueda, H.; Szejtli, J.; Fenyvesi, E. V. A.; Machida, Y.; Nagai, T., Complexation of Several Drugs with Water-Soluble Cyclodextrin Polymer. *Chem. Pharm. Bull.* **1987,** *35* (1), 282-288.

62. Nie, S.; Zhang, S.; Pan, W.; Liu, Y., In vitro and in vivo studies on the complexes of glipizide with water-soluble β-cyclodextrin-epichlorohydrin polymers. *Drug Dev. Ind. Pharm.* **2011,** *37*, 606-12.

63. Jabbari, A.; Sadeghian, H., Chapter 12 - Amphiphilic Cyclodextrins, Synthesis, Utilities and Application of Molecular Modeling in Their Design. In *Rec. Adv. Novel Drug Carrier Syst.*, Sezer, A. D., Ed. IntechOpen: London, 2012; pp 331-354.

64. Doan, V. T. H.; Takano, S.; Doan, N. A. T.; Nguyen, P. T. M.; Nguyen, V. A. T.; Pham, H. T. T.; Nakazawa, K.; Fujii, S.; Sakurai, K., Anticancer efficacy of cyclodextrin-based hyperbranched polymer nanoparticles containing alpha-mangostin. *Polym. J.* **2021,** *53* (3), 481-492.

65. Ma, M.; Li, D., New Organic Nanoporous Polymers and Their Inclusion Complexes. *Chem. Mater.* **1999,** *11* (4), 872-874.

66. Fenyvesi, É., Cyclodextrin polymers in the pharmaceutical industry. *J. Inclusion Phenom.* **1988,** *6* (5), 537-545.

67. Szeman, J.; Fenyvesi, E.; Szejtli, J.; Ueda, H.; Machida, Y.; Nagai, T., Water soluble cyclodextrin polymers: Their interaction with drugs. *J. Inclusion Phenom.* **1987,** *5* (4), 427-431.

68. Karoyo, A. H.; Wilson, L. D., Nano-Sized Cyclodextrin-Based Molecularly Imprinted Polymer Adsorbents for Perfluorinated Compounds—A Mini-Review. *Nanomaterials* **2015,** *5* (2), 981-1003.

69. Del Valle, E. M. M., Cyclodextrins and their uses: a review. *Process Biochem.* **2004,** *39* (9), 1033-1046.

70. Loftsson, T.; Hreinsdóttir, D.; Másson, M., Evaluation of cyclodextrin solubilization of drugs. *Int. J. Pharm.* **2005,** *302* (1-2), 18-28.

71. Hirose, K., A Practical Guide for the Determination of Binding Constants. *J. Inclusion Phenom. Macrocyclic Chem.* **2001,** *39* (3), 193-209.

72. Colbourne, A. A.; Meier, S.; Morris, G. A.; Nilsson, M., Unmixing the NMR spectra of similar species – vive la différence. *Chem. Commun.* **2013,** *49* (89), 10510-10512.

73. Ferrazza, R.; Rossi, B.; Guella, G., DOSY-NMR and Raman investigations on the self-aggregation and cyclodextrin complexation of vanillin. *J. Phys. Chem. B* **2014,** *118* (25), 7147-7155.

74. Simova, S.; Berger, S., Diffusion Measurements vs. Chemical Shift Titration for Determination of Association Constants on the Example of Camphor–

Cyclodextrin Complexes. *J. Inclusion Phenom. Macrocyclic Chem.* **2005,** *53* (3), 163-170.

75. Meryem, G.; Rabah, K.; Fatiha, M.; Leila, N.; Aziz, B. A.; Imane, D.; Rachid, M., Computational investigation of vanillin/β-cyclodextrin inclusion complex: Electronic and intermolecular analysis. *J. Mol. Liq.* **2021,** *321*, 114839.

76. Karathanos, V. T.; Mourtzinos, I.; Yannakopoulou, K.; Andrikopoulos, N. K., Study of the solubility, antioxidant activity and structure of inclusion complex of vanillin with β-cyclodextrin. *Food Chem.* **2007,** *101* (2), 652-658.

77. Korytkowska-Wałach, A.; Dubrawska, B.; Śmiga-Matuszowicz, M.; Bieg, T., Spectroscopic study on the inclusion complexes of β-cyclodextrin with selected metabolites of catecholamines. *J. Mol. Struct.* **2017,** *1127*, 532-538.

78. Albalasmeh, A. A.; Berhe, A. A.; Ghezzehei, T. A., A new method for rapid determination of carbohydrate and total carbon concentrations using UV spectrophotometry. *Carbohydr. Polym.* **2013,** *97* (2), 253-261.

79. Claridge, T. D. W., Chapter 10 - Diffusion NMR Spectroscopy. In *High-Resolution NMR Techniques in Organic Chemistry (Third Edition)*, Claridge, T. D. W., Ed. Elsevier: Boston, 2016; pp 381-419.

80. Fernandes, C.; Carvalho, R.; Costa, S. P. D.; Veiga, F., Multimodal molecular encapsulation of nicardipine hydrochloride by β-cyclodextrin, hydroxypropy β-cyclodextrin and triacetyl β-cyclodextrin in solution. Structural studies by ^{1}H NMR and ROESY experiments. *Eur. J. Pharm. Sci.* **2003,** *18*, 285-296.

81. Maheshwari, A.; Sharma, M.; Sharma, D., Complexation of sodium picosulphate with beta cyclodextrin: NMR spectroscopic study in solution. *J. Inclusion Phenom. Macrocyclic Chem.* **2013,** *77*.

82. Ali, S. M.; Asmat, F.; Maheshwari, A., NMR spectroscopy of inclusion complex of D-(-)-chloramphenicol with beta-cyclodextrin in aqueous solution. *Farmaco* **2004,** *59* (10), 835-8.

83. Divakar, S., Structure of a. beta.-cyclodextrin-vanillin inclusion complex. *J. Agric. Food Chem.* **1990,** *38* (4), 940-944.

84. Pîrnau, A.; Bogdan, M.; Floare, C. G. In *NMR spectroscopic characterization of β-cyclodextrin inclusion complex with vanillin*, Processes in

Isotopes and Molecules, Romania, Sept 24-26, 2009; J. Phys.: Conf. Ser.: Romania, 2009.

85. Thordarson, P., Determining association constants from titration experiments in supramolecular chemistry. *Chem. Soc. Rev.* **2011,** *40* (3), 1305-1323.

86. Claridge, T. D. W., Chapter 9 - Correlations Through Space: The Nuclear Overhauser Effect. In *High-Resolution NMR Techniques in Organic Chemistry (Third Edition)*, Elsevier: Boston, 2016; pp 315-380.

87. Alsbaiee, A.; Smith, B. J.; Xiao, L.; Ling, Y.; Helbling, D. E.; Dichtel, W. R., Rapid removal of organic micropollutants from water by a porous β-cyclodextrin polymer. *Nature* **2016,** *529* (7585), 190-194.

88. Sakurai, K.; Fujii, S.; Doan, V. T. H.; Nguyen, P. T. M.; Nguyen, V. A. T.; Pham, H. T. T. Particles, Method for Producing Particles, Drug, Method for Producing Drug, and Anti-cancer Agent. J190398T00, 2019.

89. Aminu, N.; Bello, I.; Umar, N. M.; Tanko, N.; Aminu, A.; Audu, M. M., The influence of nanoparticulate drug delivery systems in drug therapy. *J. Drug Deliv. Sci. Technol* **2020,** *60*, 101961.

90. Ferreira, L.; Campos, J.; Veiga, F.; Cardoso, C.; Paiva-Santos, A. C., Cyclodextrin-based delivery systems in parenteral formulations: A critical update review. *Eur. J. Pharm. Biopharm.* **2022,** *178*, 35-52.

91. Braga, S. S., Cyclodextrins: Emerging Medicines of the New Millennium. *Biomolecules* **2019,** *9* (12).

92. Gergely, V.; Sebestyén, G.; Virág, S. In *Toxicity studies of beta-cyclodextrin*, Proceedings of the First International Symposium on Cyclodextrins, Dordrecht, Szejtli, J., Ed. Springer: Dordrecht, 1982; pp 109-113.

93. Haimhoffer, Á.; Rusznyák, Á.; Réti-Nagy, K.; Vasvári, G.; Váradi, J.; Vecsernyés, M.; Bácskay, I.; Fehér, P.; Ujhelyi, Z.; Fenyvesi, F., Cyclodextrins in Drug Delivery Systems and Their Effects on Biological Barriers. *Sci. Pharm.* **2019,** *87* (4), 33.

94. Karthic, A.; Roy, A.; Lakkakula, J.; Alghamdi, S.; Shakoori, A.; Babalghith, A. O.; Emran, T. B.; Sharma, R.; Lima, C. M. G.; Kim, B.; Park, M. N.; Safi, S. Z.; de Almeida, R. S.; Coutinho, H. D. M., Cyclodextrin nanoparticles for diagnosis

and potential cancer therapy: A systematic review. *Front. Cell. Dev. Biol.* **2022,** *10*, 984311.

95. Doan, V. T. H.; Lee, J. H.; Takahashi, R.; Nguyen, P. T. M.; Nguyen, V. A. T.; Pham, H. T. T.; Fujii, S.; Sakurai, K., Cyclodextrin-based nanoparticles encapsulating α-mangostin and their drug release behavior: potential carriers of α-mangostin for cancer therapy. *Polymer Journal* **2020,** *52* (4), 457-466.

96. Van, D. T. H.; Anh, D. T. N.; Fujii, S.; Sakurai, K., Enhanced Binding Constant of Cyclodextrin to Alpha-mangostin in Hyperbranched Polymers. *Chemistry Letters* **2020,** *49* (10), 1144-1146.

97. Landy, D., Measuring Binding Constants of Cyclodextrin Inclusion Compounds. In *Cyclodextrin Fundamentals, Reactivity and Analysis*, Fourmentin, S.; Crini, G.; Lichtfouse, E., Eds. Springer International Publishing: Cham, 2018; pp 223-255.

98. Pessine, F.; Calderini, A.; Alexandrino, G., Review: Cyclodextrin Inclusion Complexes Probed by NMR Techniques. In *Magnetic Resonance Spectroscopy*, IntechOpen: 2012.

99. Ferrazza, R.; Rossi, B.; Guella, G., DOSY-NMR and Raman Investigations on the Self-Aggregation and Cyclodextrin Complexation of Vanillin. *The Journal of Physical Chemistry B* **2014,** *118* (25), 7147-7155.

100. Cabaleiro-Lago, C.; Nilsson, M.; Söderman, O., Self-Diffusion NMR Studies of the Host–Guest Interaction between β-Cyclodextrin and Alkyltrimethylammonium Bromide Surfactants. *Langmuir* **2005,** *21* (25), 11637-11644.

101. Gilard, V.; Trefi, S.; Balayssac, S.; Delsuc, M. A.; Gostan, T.; Malet-Martino, M.; Martino, R.; Prigent, Y.; Taulelle, F., Chapter 6 - DOSY NMR for Drug Analysis. In *NMR Spectroscopy in Pharmaceutical Analysis*, Holzgrabe, U.; Wawer, I.; Diehl, B., Eds. Elsevier: Amsterdam, 2008; pp 269-289.

102. Hrabe, J.; Kaur, G.; Guilfoyle, D. N., Principles and limitations of NMR diffusion measurements. *J. Med. Phys.* **2007,** *32* (1), 34-42.

103. Price, W. S., NMR Diffusometry. In *Modern Magnetic Resonance*, Webb, G. A., Ed. Springer International Publishing: Cham, 2017; pp 1-17.

104. Aree, T., Inclusion Scenarios and Conformational Flexibility of the SSRI Paroxetine as Perceived from Polymorphism of β-Cyclodextrin-Paroxetine Complex. *Pharmaceuticals* **2022,** *15* (1), 98.

105. Bernini, A.; Spiga, O.; Ciutti, A.; Scarselli, M.; Bottoni, G.; Mascagni, P.; Niccolai, N., NMR studies of the inclusion complex between β-cyclodextrin and paroxetine. *Eur. J. Pharm. Sci.* **2004,** *22* (5), 445-450.

106. Caira, M. R.; De Vries, E.; Nassimbeni, L. R.; Jacewicz, V. W., Inclusion of the Antidepressant Paroxetine in β-cyclodextrin. *J. Incl. Phenom. Macrocycl. Chem.* **2003,** *46* (1), 37-42.

107. Thordarson, P., Determining association constants from titration experiments in supramolecular chemistry. *Chemical Society Reviews* **2011,** *40* (3), 1305-1323.

108. D'Mello, S. R.; Cruz, C. N.; Chen, M.-L.; Kapoor, M.; Lee, S. L.; Tyner, K. M., The evolving landscape of drug products containing nanomaterials in the United States. *Nat. Nanotechnol.* **2017,** *12* (6), 523-529.

109. McNeil, S. E., Nanoparticle therapeutics: a personal perspective. *WIREs Nanomed. Nanobiotechnol.* **2009,** *1* (3), 264-271.

110. Doan, V. T. H.; Katsuki, J.; Takano, S.; Nguyen, P. T. M.; Nguyen, V. A. T.; Pham, H. T. T.; Fujii, S.; Sakurai, K., Determining the critical quality attribute for the delivery of α–mangostin by β–cyclodextrin-based nanoparticles in cancer treatment. *Polym. J.* **2023,** *55* (12), 1367-1378.

111. Thomson, J.; Liu, Y.; Sturtevant, J. M.; Quiocho, F. A., A thermodynamic study of the binding of linear and cyclic oligosaccharides to the maltodextrin-binding protein of Escherichia coli. *Biophys. Chem.* **1998,** *70* (2), 101-108.

112. Saha, S.; Roy, A.; Roy, K.; Roy, M. N., Study to explore the mechanism to form inclusion complexes of β-cyclodextrin with vitamin molecules. *Scientific Reports* **2016,** *6* (1), 35764.

113. Wszelaka-Rylik, M.; Gierycz, P., Isothermal titration calorimetry (ITC) study of natural cyclodextrins inclusion complexes with tropane alkaloids. *Therm. Anal. Calorim.* **2015,** *121* (3), 1359-1364.

114. Arti, S.; Kaur, K.; Kaur, J.; Ghosh, T. K.; Banipal, T. S.; Banipal, P. K., Host-guest interaction of trimethoprim drug with cyclodextrins in aqueous solutions:

Calorimetric, spectroscopic, volumetric and theoretical approach. *J. Mol. Liq.* **2021,** *329*, 115431.

115. Hogarth, C.; Arnold, K.; McLauchlin, A.; Rannard, S. P.; Siccardi, M.; McDonald, T. O., Evaluating the impact of systematic hydrophobic modification of model drugs on the control, stability and loading of lipid-based nanoparticles. *J. Mater. Chem. B* **2021,** *9* (48), 9874-9884.

116. Kalepu, S.; Nekkanti, V., Insoluble drug delivery strategies: review of recent advances and business prospects. *Acta Pharm. Sin. B* **2015,** *5* (5), 442-453.

117. Beg, S.; Swain, S.; Rizwan, M.; Irfanuddin, M.; Malini, D. S., Bioavailability enhancement strategies: basics, formulation approaches and regulatory considerations. *Curr. Drug Delivery* **2011,** *8* (6), 691-702.

118. Davis, M. E.; Brewster, M. E., Cyclodextrin-based pharmaceutics: past, present and future. *Nat. Rev. Drug Discovery* **2004,** *3* (12), 1023-1035.

119. Oka, N.; Matsubara, H.; Imai, T.; Yoshioka, Y.; Katsuki, J.; Fujii, S.; Nakamura, S.; Shimazawa, M.; Hara, H.; Sakurai, K., Protective effects of alpha-mangostin encapsulated in cyclodextrin-nanoparticle on cerebral ischemia. *J. Controlled Release* **2023,** *353*, 216-228.

120. McNeil, S. E., Nanoparticle therapeutics: a personal perspective. *WIREs Nanomed Nanobiotechnol.* **2009,** *1* (3), 264-271.

121. Owens, D. E.; Peppas, N. A., Opsonization, biodistribution, and pharmacokinetics of polymeric nanoparticles. *Int. J. Pharm.* **2006,** *307* (1), 93-102.

122. Irie, T.; Uekama, K., Pharmaceutical applications of cyclodextrins. III. Toxicological issues and safety evaluation. *J. Pharm. Sci.* **1997,** *86* (2), 147-162.

123. Stella, V. J.; He, Q., Cyclodextrins. *Toxicol. Pathol.* **2008,** *36* (1), 30-42.

124. Stella, V. J.; Rajewski, R. A., Sulfobutylether-β-cyclodextrin. *Int. J. Pharm.* **2020,** *583*, 119396.

125. Puskás, I.; Varga, E.; Tuza, K.; Szemán, J.; Fenyvesi, É.; Sohajda, T.; Szente, L., *Sulfobutylether-cyclodextrins: structure, degree of substitution and functional performance*. Nova Science Publishers Inc.: Hauppauge, NY, USA: 2015; Vol. 10, p 293-320.

126. Yang, Z.; Xiao, D.; Ling, K. H. J.; Tarnowski, T.; Humeniuk, R.; Parmentier, B.; Fu, Y.-H. A.; Johnson, E.; Luna, M. L.; Goudarzi, H.; Cheng, Q., The

determination of Sulfobutylether β-Cyclodextrin Sodium (SBECD) by LC-MS/MS and its application in remdesivir pharmacokinetics study for pediatric patients. *J. Pharm. Biomed. Anal.* **2022,** *212*, 114646.

127. Sakurai, K.; Fujii, S.; Van Doan, T. H.; Nguyen, T. M. P.; Nguyen, T. V. A.; Pham, T. T. H. Particles, method for producing particles, drug, method for producing drug, and anti-cancer agent. 2022.

128. Doan, V. T. H.; Katsuki, J.; Takano, S.; Nguyen, P. T. M.; Nguyen, V. A. T.; Pham, H. T. T.; Fujii, S.; Sakurai, K., Determining the critical quality attribute for the delivery of α–mangostin by β–cyclodextrin-based nanoparticles in cancer treatment. *Polym. J.* **2023,** *55*, 1367-1378.

129. Christoforides, E.; Papaioannou, A.; Bethanis, K., Crystal structure of the inclusion complex of cholesterol in β-cyclodextrin and molecular dynamics studies. *Beilstein J. Org. Chem.* **2018,** *14*, 838-848.

130. Dai, Y.; Zhong, J.; Li, J.; Liu, X.; Wang, Y.; Qin, X., Interaction mechanism of cholesterol/β-cyclodextrin complexation by combined experimental and computational approaches. *Food Hydrocoll.* **2022,** *130*, 107725.

131. Pritchett-Corning, K.; Hashway, S.; Suckow, M., *The Laboratory Mouse (3rd ed.)*. CRC Press: 2023.

132. Van, D. T. H.; Anh, D. T. N.; Fujii, S.; Sakurai, K., Enhanced binding constant of cyclodextrin to alpha-mangostin in hyperbranched polymer. *Chem. Lett.* **2020,** *49* (10).

133. Doan, A. T. N.; Sakurai, K., Unraveling the molecular mechanism of the interaction between cyclodextrin-based nanoparticles (CDNPs) and paroxetine hydrochloride. *Bull. Chem. Soc. Jpn.* **2024,** *97* (4).